Re-engineering of acetyl coenzyme A metabolism prevents senescence in budding yeast

Hanane Hadj-Moussa[1], Megan Ulusan[1], Dorottya Horkai[1,2], Mohammed Kamran Afzal Mirza[1] and Jonathan Houseley[1,*]

[1] Epigenetics Programme, Babraham Institute, Cambridge, United Kingdom

[2] Current address: ZOMP, Cavendish Laboratory, JJ Thomson Avenue, Cambridge, CB3 0HE, UK

* Corresponding Author: jon.houseley@babraham.ac.uk

ORCIDs:

Hanane Hadj-Moussa: 0000-0002-3338-9046

Megan Ulusan: 0009-0001-0569-3403

Dorottya Horkai: 0000-0001-9430-1864

Mohammed Kamran Afzal Mirza: 0009-0008-2467-4882

Jon Houseley: 0000-0001-8509-1500

Abstract

Although lifespan has long been the focus of ageing research, the need to enhance healthspan - the fraction of life spent in good health - is a more pressing societal need. Caloric restriction improves healthspan across eukaryotes but is unrealistic as a societal intervention. Here, we describe the rewiring of a highly conserved nutrient sensing system to prevent senescence onset and declining fitness in budding yeast even when aged on an unrestricted high glucose diet. We show that AMPK activation can prevent the onset of senescence by activating two pathways that remove excess acetyl coenzyme A from the cytoplasm into the mitochondria - the glyoxylate cycle and the carnitine shuttle. However, AMPK represses fatty acid synthesis from acetyl coenzyme A, which is critical for normal cellular function and growth. AMPK activation therefore has positive and negative effects during ageing. Combining AMPK activation with a point mutation in fatty acid synthesis enzyme Acc1 that prevents inhibition by AMPK (the A2A mutant) allows cells to maintain fitness late in life without reducing the mortality associated with advanced age. Our research shows that ageing in yeast is not intrinsically associated with loss of fitness, and that metabolic re-engineering allows high fitness to be preserved to the end of life.

Introduction

Traditional conceptions of ageing generally implicate a progressive accumulation of damage leading to systemic degradation in performance until death, with evolutionary pressures acting to maximise early life fitness and fecundity at the expense of ageing health [1-3]. The healthspan problem – the societal need to increase the fraction of human life spent in good health – is almost insoluble under such models, since poor health late in life is an inevitable intermediate stage in the damage accumulation leading to death. In support of this, most lifespan-extending mutations in *C. elegans* proportionately extend the organismal survival function and do not improve healthspan [4,5]. However, ageing is not uniform across populations and from yeast to humans it is clear that some members of any population maintain excellent fitness and low senescence late in life [6-8]: increasing the population fraction of such low-senescence individuals is a primary aim of ageing research. Interventions such as caloric restriction and mTOR inhibition can improve healthspan [9-13], but caloric restriction is an unrealistic societal intervention and mTOR inhibition has side effects, so new interventions are required. The recent discovery that GLP1 agonists improve markers of ageing health has engendered optimism that other pharmacological pathways to improving ageing health are possible, and more widely that manipulating food intake or physiological responses to diet could be beneficial without strict caloric restriction [14-16].

Replicative ageing of the budding yeast *Saccharomyces cerevisiae* is a widely used model of ageing, and provides a simple model for ageing health. Budding yeast cells divide asymmetrically into a mother cell and a daughter cell, with the mother cell undergoing only a limited number of divisions before permanently exiting the cell cycle [17]. Mother cells maintain a rapid and uniform cell cycle for most of their replicative lifespan but the cell cycle often slows dramatically in the last few divisions indicating loss of fitness [17-19], an effect known as 'senescence' following the classical definition of the term 'senescence' to denote a period of very low fitness at the end of life. A sharp transition termed the senescence entry point (SEP) marks the change from rapid to slow, heterogeneous cycling, and is coincident with the appearance of apparently pathological markers [19,20]. Not all cells senesce, and populations are extremely heterogeneous in some experimental systems with individual cells following either a short-lived trajectory marked by an early SEP and accumulated foci of a mitochondrial Tom70-GFP marker when present, or a long-lived trajectory with little evidence of senescence [8,21,22]. We recently discovered that changing yeast from a glucose diet to a galactose diet without caloric restriction allowed all cells to age without undergoing senescence; this did not extend lifespan and most cells maintained youthful fitness to the end of life [23]. The mechanistic basis for this healthspan extension remains unknown but respiration was required, and forcing mitochondrial biogenesis in cells ageing on a normal glucose diet caused part of the population to follow a low senescence trajectory.

In both yeast and mammalian cells, mitochondrial biogenesis is controlled by AMPK (AMP-activated kinase), a well-characterised element of the response to poor nutrient availability that reconfigures energy utilisation through both modification of metabolic enzymes and remodelling of gene expression programmes (reviewed in [24,25]). AMPK enhances energy production by increasing respiration, mobilising internal energy stores, inducing autophagy and moderating fatty acid biosynthesis, and is regulated in response to low energy state based on the AMP/ADP ratio as well as damage to DNA, lysosomes and mitochondria [26-29]. Due to its

pivotal position in the response to low energy and maintenance of cellular homeostasis, AMPK has long been a focus of efforts to understand caloric restriction [30,31], and is required for the beneficial effects of caloric restriction in yeast, worms and in flies [32-34]. Overexpression of the AMPK catalytic subunit extends lifespan in *C. elegans* and *D. melanogaster*, and high doses of the indirect AMPK activator metformin can even extend lifespan and healthspan in mice [35-39]. However, many studies of metformin have not observed beneficial effects in mice or humans, and although metformin activates AMPK in *D. melanogaster* this has no effect on lifespan [40,41].

Caloric restriction robustly extends lifespan in budding yeast [42-44], but AMPK has different effects on yeast lifespan depending on the ageing paradigm employed, shortening replicative lifespan but extending chronological lifespan [45,46]. Yeast AMPK is a central regulator of energy metabolism, and despite responding to glucose levels rather than sensing AMP:ADP ratio, shares close mechanistic and functional parallels with its counterpart in higher eukaryotes. In budding yeast, AMPK is composed of a catalytic α subunit Snf1, a regulatory β subunit (Sip1, Sip2 or Gal83) and an accessory γ subunit Snf4 (reviewed in [47]). It is activated by phosphorylation at a structurally conserved site, Thr210, by kinases Sak1, Elm1 and Tos3, and is regulated in response to glucose availability through Snf1 dephosphorylation, pH and subunit binding [48-50]**.** AMPK negatively regulates growth signalling pathways by phosphorylating adenylate cyclase to dampen PKA signalling, and Pib2 and Sch9 to reduce mTOR signalling at multiple steps [51,52]. Conversely, AMPK promotes transcription of genes for mitochondrial biogenesis and alternative carbon source utilisation through inhibition of the transcriptional repressor Mig1 and activation of the transcription factor Cat8 [53,54].

Lipid synthesis is a key target of AMPK. Cytoplasmic acetyl coenzyme A is the building block for lipids, being processed into malonyl coenzyme A by acetyl coenzyme A carboxylase (ACC) to initiate fatty acid synthesis or into hydroxymethylglutaryl coenzyme A for synthesis of isoprenoids including cholesterol and ergosterol. Sources of cytoplasmic acetyl coenzyme A vary: in mammalian cells this is primarily generated by ATP citrate lyase (ACLY) from mitochondrially exported citrate, with a smaller fraction (depending on diet, cell type/state and local conditions) made from acetate by acetyl coenzyme A synthase (ACS) [55-57]. In budding yeast, cytoplasmic acetyl coenzyme A is also generated by ACS from acetate, which is available through oxidation of the fermentation intermediate acetaldehyde [58]. Irrespective of acetyl coenzyme A source, the synthesis of fatty acids is controlled by AMPK through inhibitory phosphorylation of ACC: this has been described for budding yeast Acc1, for *Drosophila* ACC and for mammalian ACC1/ACC2, forming a highly conserved mechanism to suspend energy storage in fatty acids under low energy conditions where fatty acid catabolism is initiated [59-62].

Here we build on our finding that a galactose diet suppresses senescence in yeast by investigating the effect of AMPK activation. We show that AMPK prevents senescence in a subset of cells by redirecting acetyl coenzyme A flux, and that AMPK activation combined with disruption of the AMPK/ACC regulatory system is sufficient for yeast cells to avoid the SEP and maintain high fitness late in life when aged on a normal, high glucose diet.

Results

Increased AMPK activity suppresses senescence in a subset of cells

S. cerevisiae metabolises both glucose and galactose by fermentation, but AMPK is only active and necessary for growth on galactose [63,64]. Given that AMPK is required for the suppression of senescence during ageing on galactose [23], we asked whether activation of AMPK during ageing on glucose could recapitulate the benefits of ageing on galactose. For this study, we compared log phase populations of *S. cerevisiae* (average age 0-1 generation) to purified cohorts aged on rich glucose media for 24 or 48 hours (average replicative ages ~12 and ~18 generations, at which points cells are ~95% and ~30% viable respectively). Experiments were performed in batch culture with diploid cells using the well-characterised mother enrichment program (MEP) system to enrich aged cells, combined with cell wall biotin labelling for purification as described [23,65]. Cells carried Tom70-GFP as a marker of senescence [8,19], were co-stained for bud scars using WGA to quantify replicative age [66-68], and an Rpl13a-mCherry control marker that is unaffected by senescence was also included in most experiments [69]. Cell populations were analysed by flow cytometry, allowing sub-populations with different replicative ages and different senescence status to be identified (Figure 1A).

AMPK was activated on glucose by constitutive over-expression of the upstream kinase Sak1 using a P_{GPD} promoter as described [70,71] , resulting in a 12-fold increase in *SAK1* mRNA at log phase that dropped to 5-fold by 48 h (Figure S1A). After 48 h of ageing, the average intensity of senescence marker Tom70-GFP in P_{GPD}-*SAK1* was significantly though subtly reduced relative to wild type, while replicative age based on WGA was occasionally but not always higher, with Rpl13a being unchanged (Figure 1B, Figure S1B). The variability of these bulk measurements stemmed from the emergence of a new sub-population of aged cells with low Tom70-GFP and high WGA (Figure 1A,C top left quadrant). Whereas the Tom70-GFP senescence marker increased substantially from log to 48 h across the whole population of wild-type cells, consistent with almost all cells becoming senescent, ~30% of cells overexpressing Sak1 formed a discrete sub-population with lower Tom70-GFP. This sub-population has a higher replicative age (marked by WGA) as non-senescent cells cycle rapidly throughout life rather than slowing down after the SEP. Low Tom70-GFP and high replicative age at 48 h therefore mark a subpopulation of cells on a low senescence trajectory, which was observed consistently across experiments (Figure 1C right).

We previously noted that respiration is required to avoid senescence on galactose [23], and asked whether inducing respiration on glucose underpins the low senescence phenotype of AMPK-activated cells (Figure 1D). Abrogating the electron transport chain through removal of Complex IV-component Cox9 prevented the emergence of the low senescence population in P_{GPD}-*SAK1,* with most P_{GPD}-*SAK1 cox9*Δ cells being in the high Tom70-GFP, lower WGA population at 48 h (Figure 1E). Deletion of *COX9* may limit lifespan and prevent cells reaching the high WGA, low Tom70-GFP state, however this would yield a low/mid WGA, low Tom70-GFP population which we also did not observe. The mechanism by which P_{GPD}-*SAK1* promotes ageing health therefore requires the electron transport chain, but it was unclear why the limited shift from fermentation to respiration caused by AMPK activation in young cells would have such a strong effect given that respiration is highly induced with age even in wild type [70,72]. Furthermore, although aerobic respiration during growth on glucose should involve mitochondrial uptake of pyruvate derived from glycolysis [73], loss of Mpc1, the major subunit of the mitochondrial pyruvate transporter in combination with P_{GPD}-*SAK1* had no effect on the low-senescence sub-population (Figure 1E).

Therefore, AMPK activation during growth on glucose allows part of the population to age on a low senescence trajectory. This depends on the electron transport chain, but does not require

pyruvate derived from glycolysis to enter mitochondria, raising questions as to the substrate for respiration.

AMPK activation reduces senescence onset through acetyl coenzyme A metabolism

Overexpression of *SAK1* reduced the known dysregulation of gene expression with ageing (Figure S2A), despite AMPK being a transcriptional activator for many of the most dysregulated genes [67,74-77]. However, *SAK1* overexpression alone does not overcome glucose repression [71], so only 21 genes (enriched for respiration and related GO terms) were significantly upregulated at log phase in P_{GPD}-*SAK1*, and the changes in expression were not large (only two genes apart from *SAK1* were increased >3-fold)(Figure 2A, top). A larger effect was observed in aged P_{GPD}-*SAK1* cells: 472 genes were significantly different from wild type ($p<0.01$), of which the upregulated genes (74%) were enriched for GO terms related to respiration and cytoplasmic translation, while the downregulated genes shared no significant GO enrichments. Only 17 genes were substantially different (>3-fold - 8 down, 9 up including *SAK1*, Figure 2A bottom). The 8 down-regulated genes shared no apparent functional connection, but the 9 up-regulated genes included all 5 of a co-regulated gene set crucial for re-direction of acetyl coenzyme A into gluconeogenesis via the glyoxylate cycle: *MLS1*, *ICL1*, *PCK1, SFC1* and *FBP1* (Figure 2B)[78,79], and three of these were also significantly and substantially upregulated at 24 h (Figure S3B). This pathway is not used during growth on glucose, though plentiful acetyl coenzyme A is synthesised from acetaldehyde, it is required during growth on carbon sources such as ethanol and acetate when acetyl coenzyme A becomes the feedstock for gluconeogenesis and associated anabolic pathways (Figure 2B).

Mls1 and Icl1 act in the glyoxylate cycle (Figure 2C, left), which converts cytoplasmic or peroxisomal acetyl coenzyme A into succinate: Sfc1 transports succinate into mitochondria for dehydrogenation by succinate dehydrogenase (Complex II of the electron transport chain), and shuttles the resulting fumarate back to the cytoplasm for conversion to oxaloacetate; Pck1 converts oxaloacetate to phosphoenolpyruvate, initiating the gluconeogenesis pathway which is driven by Fbp1 (Figure 2B). These genes are amongst many whose mRNA levels are reported to increase with age, but the effect of P_{GPD}-*SAK1* is very specific to this set [80,81]. Deletion of *MLS1* or *SFC1* significantly reduced the low senescence sub-population in P_{GPD}-*SAK1,* identifying acetyl coenzyme A metabolism as a key element in the onset of senescence (Figure 2D).

Acetyl coenzyme A can also be transported from the cytoplasm into mitochondria for use in the TCA cycle after conjugation to carnitine by carnitine acetyl transferases (Figure 2C, right). *S. cerevisiae* cannot synthesise carnitine but it is available from the YPD media, which allows this carnitine shuttle to operate in parallel with the glyoxylate cycle [82-84]. Although multiple carnitine acetyl transferases exist outside mitochondria, the carnitine shuttle depends on the mitochondrial carnitine acetyltransferase Cat2 to convert acetyl carnitine back to acetyl coenzyme A. Deletion of *CAT2*, combined with deletion of *MLS1* to abrogate the glyoxylate cycle, almost completely suppressed the effect of P_{GPD}-*SAK1* with very few cells achieving the high WGA, low Tom70-GFP phenotype at 48h, showing that pathways which process acetyl coenzyme A for mitochondrial import are critical in avoiding senescence (Figure 2E). Transport of cytoplasmic acetyl coenzyme A into mitochondria fuels respiration during growth on acetate and ethanol and most likely fuels respiration in P_{GPD}-*SAK1* cells ageing on glucose; conversely respiration is required for the glyoxylate cycle and for the TCA cycle, linking the requirements for respiration and acetyl coenzyme A metabolism in suppressing senescence. Our findings

therefore show that control of cytoplasmic acetyl coenzyme A metabolism is a key part of the mechanism by which AMPK activation promotes ageing on a low senescence trajectory.

Combining AMPK activity and fatty acid synthesis to avoid senescence

Cytoplasmic acetyl coenzyme A is the building block for fatty acids, which are indispensable for growth and survival. AMPK controls fatty acid production by phosphorylating two serines in yeast Acc1 to inhibit the first step in fatty acid synthesis from acetyl coenzyme A, with Ser1157 being the main regulatory site (Figure 3A) [85,86]. We hypothesised that Acc1 inhibition may limit the positive effects of AMPK activation by throttling the production of fatty acids during growth on rich, high glucose media. To test this, we combined P_{GPD}-*SAK1* with an *acc1*^{S1157A} mutation that prevents Acc1 inactivation by AMPK, thereby creating the A2A mutant.

Young A2A cells proliferate equivalently to wild-type cells in liquid culture (Figure S3A), and do not have an extended replicative lifespan (Figure S3B), but show a significant and substantial increase in the low senescence population relative to P_{GPD}-*SAK1* (Figure 3B). Separate analysis of Tom70-GFP and WGA reveals that A2A and P_{GPD}-*SAK1* populations are equivalent on average at 24 hours, but A2A shows consistently lower Tom70-GFP and higher WGA by 48 h (Figure 3C), whereas the control marker Rpl13a-mCherry, which labels a ribosomal protein that is stable across SEP state, is unaffected (Figure S3C). Population measurements of Tom70-GFP and WGA do vary between experiments, but differences were consistent over many experiments (Figure S3D, n>25), and bud scar counts confirmed that A2A cells reach a higher age than wild-types at 48 h so the observed difference in WGA intensity does not simply result from differences in staining (Figure S3E). The bulk population measurements of Tom70-GFP and WGA in A2A proved consistently different from wild type because the majority of cells form a single, low senescence population rather than being split across two populations as in P_{GPD}-*SAK1*. The combination of AMPK activation and unfettered fatty acid synthesis therefore allows the majority of cells to age without senescence.

A2A cells cultured for 40 hours reached a comparable average replicative age to wild-type at 48 h, and at this point form a very clear low senescence population, confirming that SEP onset is delayed or absent in age-matched cells (Figure 3D). This reduction of senescence occurs despite viability of A2A cells being lower at 40 h than wildtype at 48 h based on colony forming ability (Figure 3E). Importantly, at 40 h >50% of A2A cells were in the low Tom70-GFP, high age population even though <20% are viable, meaning that many cells reach the end of their replicative lifespan without passing the SEP.

Tom70-GFP and WGA signals are only indirect indicators of cell fitness, whereas the speed at which individual cells form colonies is a direct physiological measure of fitness (Figure 3F). While young A2A cells formed slightly smaller colonies than wild-type cells, colonies formed by aged A2A cells were much larger than those formed by wild type cells of equivalent replicative age. Indeed, aged A2A cells formed colonies of similar size to young A2A cells showing equivalent fitness, whereas most aged wild-type cells divided only once or not at all across the 24-hour assay period, showing that A2A cells maintain high fitness late in life whereas the fitness of aged wild-type cells is very low. Importantly, only viable cells that eventually formed colonies after 3 days were included in this analysis, so the non-dividing aged wild-type cells were viable but had a cell division time greater than 24 hours. Comparing fitness of wild type, *acc1*^{S1157A}, P_{GPD}-*SAK1* and A2A at a fixed 48 h time point revealed that A2A maintained the best

fitness despite also having the highest median age, while P_{GPD}-*SAK1* showed variable fitness and *acc1*^{S1157A} was similar to wild type (Figure 3G). It is worth noting that colony formation by log phase cells carrying the P_{GPD}-*SAK1* construct was consistently slower than wildtype (5% longer doubling time on average) even if this does not manifest in liquid growth assays.

AMPK is the best characterised Sak1 substrate but at least one more exists [87]**.** To ensure that suppression of senescence in A2A arises from AMPK activation, we generated two additional mutants - A2B and A2C, that do not contain P_{GPD}-*SAK1* and instead carry activating point mutations in the AMPK catalytic subunit Snf1 combined with *acc1*^{S1157A}. Both A2B (*snf1*^{L183I} *acc1*^{S1157A}) and A2C (*snf1*^{T210D} *acc1*^{S1157A}) caused a significant increase in the low senescence population at 48 h (Figure 3H). Separate analysis of Tom70-GFP and WGA showed that Tom70-GFP was significantly decreased whereas WGA was not increased (Figure S3F), indicating that constitutive activation of AMPK has a similar impact to Sak1 overexpression, but that this complete dysregulation of AMPK adversely affects viability late in life.

These experiments show that the beneficial effects of AMPK activation during ageing can be increased substantially if inhibition of Acc1 is prevented, such that normal fatty acid biosynthesis is maintained. A combination of increased AMPK activation with normal fatty acid synthesis yields a robust low senescence ageing phenotype and high late life fitness without decreasing the mortality rate.

The molecular basis of reduced senescence in P_{GPD}-SAK1 *and A2A*

To understand why senescence is reduced in the A2A mutant, we first tested whether the genetic dependencies of senescence are equivalent to P_{GPD}-*SAK1*. Loss of *COX9* abrogated the low senescence population in A2A at 48 h (Figure 4A), showing the expected dependence on respiration, and similarly *cat2*Δ *mls1*Δ dramatically reduced the benefit of A2A (Figure 4B), showing that AMPK activation suppresses senescence through the same mechanism in P_{GPD}-*SAK1* and A2A. We then investigated why acetyl coenzyme A transport from the cytoplasm into mitochondria is beneficial, and why this benefit is increased by Acc1 activity.

Cytoplasmic acetyl coenzyme A is the substrate for multiple metabolic pathways, but also regulates AMPK through a Sip2-dependent feedback mechanism that inactivates AMPK when acetyl coenzyme A availability is high (Figure 4C) [88]. It was therefore necessary to delete *SIP2* before perturbing acetyl coenzyme A metabolism to isolate these pathways from AMPK feedback regulation. This had little effect on the system: P_{GPD}-*SAK1* substantially increased the low senescence population in *sip2*Δ just as in wild type albeit from a lower starting point (Figure 4D), and a subset of these cells showed higher fitness at 48 h (Figure S4A). However, the average population age did not increase (Figure S4B), likely because *sip2*Δ limits lifespan [46].

We asked whether the protective effect of mitochondrial acetyl coenzyme A import by the glyoxylate cycle and the carnitine shuttle reflects a positive role for acetyl coenzyme A imported into mitochondria, or a toxic effect of acetyl coenzyme A in the cytoplasm. To reduce the supply of cytoplasmic acetyl coenzyme A, we deleted *ALD6,* which encodes the primary aldehyde dehydrogenase active during growth on glucose (Figure 4C) [89,90]. If mitochondrial acetyl coenzyme A import were beneficial then reducing acetyl coenzyme A supply should increase senescence, but instead the low senescence population increased in *ald6*Δ *sip2*Δ P_{GPD}-*SAK1* showing that high cytoplasmic acetyl coenzyme A availability promotes senescence (Figure 4E).

Next, we asked whether depletion of cytoplasmic acetyl coenzyme A by the glyoxylate cycle and carnitine shuttle (as well as by Acc1) impacts AMPK activity through Sip2-mediated feedback. Sip2 is a negative regulator of AMPK which binds to AMPK when Sip2 is acetylated by the histone acetyltransferase NuA4 [88], and bulk histone acetylation is reduced in A2A as others have reported when manipulating acetyl coenzyme A availability, implying that less acetyl coenzyme A is available to histone acetyltransferases in A2A (Figure S4C) [91]. However, *acc1*^{S1157A} increased the low senescence population relative to P_{GPD}-*SAK1* in a *sip2*^{3R} background which mimics the hypoacetylated state that cannot associate with AMPK, showing that the low senescence phenotype of A2A does not arise by preventing Sip2-mediated feedback from deactivating AMPK (Figure S4D). Similarly, the *sip2*^{3Q} mutation, which mimics hyperacetylated Sip2 and causes constitutive association of Sip2 with AMPK, does not reduce the low senescence population in A2A, so AMPK activity is sufficient to suppress senescence even with Sip2 bound (Figure S4E).

We then probed the role of Acc1, using the *sip2*Δ background for consistency with the *ALD6* experiment above, after confirming that *acc1*^{S1157A} increases the low senescence population in *sip2*Δ P_{GPD}-*SAK1* just as in wild type and *sip2*^{3R} (Figure 4E). We considered three mechanisms for the beneficial effect of Acc1: enhanced depletion of cytoplasmic acetyl coenzyme A in concert with the carnitine shuttle and glyoxylate cycle; synthesis of fatty acids if these are limiting during ageing; or mTOR inhibition mediated by the direct product of Acc1, malonyl coenzyme A, which was recently identified as an mTOR inhibitor [92,93]. To separate these possibilities, we supplemented *sip2*Δ P_{GPD}-*SAK1* with 0.04% oleic acid (a monounsaturated fatty acid that is liquid at 30°C and is solubilised by 0.04% Tween 80), a low dose of the fatty acid synthase inhibitor cerulenin which causes accumulation of malonyl coenzyme-A, or a high dose of cerulenin combined with oleic acid. This latter condition allows greater malonyl coenzyme A accumulation while compensating for the growth defect caused by severe fatty acid synthesis inhibition. Cerulenin treatment drastically limited ageing even at low dose, whereas oleic acid supplementation substantially increased the low senescence population at 48 h, with the combination having an intermediate effect (Figure 4F). This shows that in *sip2*Δ P_{GPD}-*SAK1*, fatty acid supplementation is very beneficial, malonyl-coenzyme A accumulation has little effect and cells are extremely sensitive to fatty acid starvation. The fact that the low senescence phenotype of *sip2*Δ P_{GPD}-*SAK1 acc1*^{S1157A} (*sip2*Δ A2A) can be recapitulated in *sip2*Δ P_{GPD}-*SAK1* by fatty acid supplementation shows that the principal role of *acc1*^{S1157A} is to prevent fatty acid starvation when AMPK is activated rather than to remove cytoplasmic acetyl coenzyme A. None of the treatments had a strong impact on Tom70-GFP, with increases in the low Tom70-GFP, high WGA population being driven almost entirely by increased WGA (Sup Figure S4G), meaning that the strongest effect of fatty acid supplementation was to overcome an inability of *sip2*Δ P_{GPD}-*SAK1* cells to reach a high age in 48 h.

After validating this effect by bud scar counting (Figure S4F), we asked whether oleic acid supplementation also reduced senescence in wild type, P_{GPD}-*SAK1* and A2A. The effects were most dramatic in wild type, with the low senescence population increasing 2.5-fold through decreased population average Tom70-GFP and increased WGA (Figure 4G,S4G). The low senescence population in P_{GPD}-*SAK1* also almost doubled with oleic acid supplementation, whereas oleic acid only had a small, non-significant effect in A2A (Figure 4G). This is consistent with our initial hypothesis that fatty acid deficiency limits the benefits of AMPK activation, but further shows that fatty acids are limiting for wildtype cells during ageing. At 48 h the fitness of wildtype cells supplemented with oleic acid increased dramatically, P_{GPD}-*SAK1* cells improved somewhat while fitness was significantly but not substantially decreased in A2A (Figure 4H). In fact, the oleic acid supplemented wild-type cells were on average fitter than the mutants, which

likely reflects the decrease in baseline fitness caused by P_{GPD}-*SAK1*, which is also visible in young cells. This result shows that a subset of cells in which AMPK is activated fail to follow the low senescence trajectory because of fatty acid starvation that can be compensated by the *acc1*^{S1157A} mutation or by oleic acid supplementation. However, the results for wild type are more complicated as flow cytometry indicates that many cells undergo senescence whereas by fitness assay all oleic acid supplemented wildtype cells are extremely fit. This difference emerges because flow cytometry also considers dead cells whereas the fitness assay only includes cells that are still viable at 48 h. In other words, more wild-type cells lose viability before 48 h with high senescence than for either of the mutants, but those which do survive to 48 h are very fit. These cells which lose viability early through senescence are likely those which are rescued by AMPK activation.

Overall, our results show that the availability of fatty acids and mitochondrial processing of acetyl coenzyme A are both critical for ageing health in yeast, with A2A simultaneously achieving both sufficient fatty acid synthesis and titration of excess acetyl coenzyme A.

Discussion

Here we have described a core system that underlies maintenance of fitness during replicative ageing in budding yeast. We find that mitochondrial uptake of acetyl coenzyme A driven by AMPK, combined with ongoing cytoplasmic fatty acid synthesis, together ensure that cells rarely enter senescence. This is achieved without reducing age-linked mortality and with little effect on the fitness of cells when young, showing that lifespan and healthspan are separable and that high fitness can be maintained to the end of life, at least in budding yeast.

The aim of our study was to determine whether and how loss of fitness with age can be prevented on a normal diet. Our findings reveal an unexpected balance in the central pathway of acetyl coenzyme A metabolism when yeast cells are aged under continuously high nutrient conditions: sufficient acetyl coenzyme A must be provided for fatty acid synthesis, but excess cytoplasmic acetyl coenzyme A must also be removed (Figure 5). Most cells fail to meet one or other of these conditions during ageing, which results in senescence onset. Ectopic AMPK activation under high nutrient availability can prevent senescence in some cells by reducing cytoplasmic acetyl coenzyme A availability, but AMPK also limits fatty acid production by inhibiting Acc1. Only when Acc1 inhibition is removed are the full benefits of AMPK activation achieved: excess acetyl coenzyme A is removed while fatty acid synthesis continues unimpeded (Figure 5). One implication of this model is that any change which subtly reduces glycolytic flux towards acetyl coenzyme A will be beneficial for ageing; caloric restriction has this effect, as does growth on galactose or redirection of glycolytic flux towards the shikimate pathway [94,95]; however this is a balance as glycolytic flux must remain sufficient for fatty acid synthesis as well as many other functions.

AMPK is broadly considered to have a pro-longevity effect, however the benefits of AMPK activation under normal diets are limited, and some studies in budding yeast conversely found that AMPK activity is negative for lifespan [80,96]. Our work shows that both positions are true, with AMPK having both beneficial and detrimental impacts through acetyl coenzyme A metabolism under nutrient replete conditions. It is not too surprising that issues arise when AMPK is ectopically activated on high glucose given that AMPK is a central energy regulator that evolved to manage metabolism under low nutrient conditions, and it is perhaps more surprising that a

single point mutation largely corrects these issues, providing optimism that the benefits of AMPK activation could also be maximised in higher eukaryotes.

Unfortunately, we do not yet understand why metabolic differences lead to the loss of fitness that defines senescence in yeast, or indeed to the changes in molecular markers linked to senescence. It is becoming clear that multiple seemingly unrelated pathways promote senescence, and which pathway dominates is highly dependent on the experimental system used [8,20,22,97,98]. The SEP in yeast was originally characterised in microfluidic assays, and substantial evidence links senescence onset to accumulation of ERCs initiated by the replication fork barrier protein Fob1 [19,20,98]. In contrast, ERC accumulation is completely unrelated to Tom70-GFP or to fitness loss during ageing in the batch culture system employed here, and ERC accumulation does not depend on Fob1 [23,99,100]. Instead, senescence onset in batch culture is sensitive to metabolic changes such as a galactose diet or acetyl coenzyme A processing; the galactose diet has no effect on cells in microfluidic systems and similarly the impact of caloric restriction has remained controversial, so we do not necessarily expect A2A to prevent senescence in microfluidic systems [101,102]. Why there should be such differences between *S. cerevisiae* replicative ageing systems is unclear, but the environments are very different: in microfluidics, cells are unlabelled and provided with constant fresh media but are under substantial physical pressure from the fluid flow; in batch culture, cells are biotin labelled which may damage the cell wall or receptors but are then aged under only a mild agitation. Oxygenation will be higher in batch culture, and media conditions change as the cells age, both of which may be important [103-105]. It is worth noting that our findings parallel studies of yeast chronological ageing which have highlighted the importance of respiration and lipid synthesis, though chronological ageing measurements are performed in glucose-depleted conditions and it has been difficult to translate these findings to ageing under high nutrient availability [32,91,106]. Whatever the root of the difference, ageing in batch culture allows the exploration of different aspects of ageing biology while avoiding the influence of ERCs, which are important in yeast but do not accumulate during ageing in animals.

It is in this context of the unknown and multiple causes of senescence that we must consider one surprising outcome of our research: while it makes perfect sense that fatty acid supplementation prevents senescence in cells with activated AMPK, it is not clear why this should be almost as effective in wild type. Acetyl coenzyme A production should be high in wild-type cells and Acc1 uninhibited so fatty acid synthesis should be substantial. Indeed, fatty acids accumulate in lipid droplets during ageing of MEP wild types [95]. One intriguing possibility is that wild type cells are defective in forming monounsaturated fatty acids such as oleic acid, which make up 70-80% of fatty acids in budding yeast [107]. Ole9, the single and essential fatty acid desaturase in yeast, is iron dependent, and loss of iron homeostasis has been previously characterised in yeast ageing [22,108,109]. Whether SAK1 overexpression or A2A normalises iron metabolism remains to be determined, but this connection hints at an overarching ageing mechanism in yeast.

Although the AMPK-Acc1 regulatory system is conserved from yeast to humans, the source and fate of cytoplasmic acetyl coenzyme A are different and the combination of AMPK activation with lipid supplementation is unlikely to be effective in human cells. In yeast, both the glyoxylate cycle and carnitine acetyltransferase can efficiently shuttle cytoplasmic acetyl coenzyme A into mitochondria - this is required for growth on acetate and ethanol. Human cells lack the glyoxylate cycle and evidence for cytoplasmic carnitine acetyltransferase activity is very limited [110], meaning that acetyl coenzyme A in the cytoplasm has no simple path into

mitochondria. The only major route available is lipid synthesis to palmitoyl coenzyme A followed by carnitine-dependent transport into mitochondria for oxidation. Ectopic activation of AMPK under high nutrient availability would promote lipid catabolism but inhibit lipid synthesis through ACC1/2 phosphorylation. Preventing inhibition of ACC1/2 by AMPK is ineffective as ACC2 also prevents fatty acid catabolism so fatty acid synthesis and storage increase, resulting in non-alcoholic fatty liver disease [111]. However, we suggest that activation of AMPK while selectively preventing AMPK inhibition of ACC1 alone may allow a futile cycle of fatty acid synthesis and degradation to emerge that limits cytoplasmic acetyl coenzyme A availability and ensures an adequate but not excessive supply of fatty acids. More generally, due to the high conservation of the regulatory networks we have associated with age-linked loss of fitness in yeast, we are optimistic that manipulation of acetyl-coenzyme A metabolism may provide a pathway to improve ageing health in mammals.

Materials and Methods

Detailed and updated protocols are available at https://www.babraham.ac.uk/our-research/epigenetics/jon-houseley/protocols.

Yeast strain construction, culture and labelling

Yeast deletion mutants and fusion constructs were constructed by standard methods and are listed in S1 Table, oligonucleotide sequences are given in S2 Table. Plasmid templates were pFA6a-GFP-KanMX4, pYM-N14, pAW8-mCherry, pFA6a-HIS3 and pFA6a-URA3 [112-114]. To create the *acc1*^{S1157A} point mutation, *ACC1* was amplified with ACC1 F3/R3 and cloned in pRS314, then the S1157A mutation introduced by site directed mutagenesis. MEP **a** ±Kan-P_{GPD}-*SAK1* cells carrying this plasmid were transformed with pGSKU [115] amplified with ACC1 CORE UP45 1 and ACC1 CORE DN45 2 to replace the chromosomal ACC1 S1157 codon with a CORE cassette flanked on each side by I-*Sce*I sites. Cells were plated on YPGal to induce I-*Sce*I then FOA to select for loss of the CORE cassette, then TRP negative cells lacking the pRS314-*acc1*^{S1157A} plasmid were verified by sequencing. *sip2*^{3R} and *sip2*^{3Q} were constructed by a simpler method as *SIP2* is not an essential gene: a CORE cassette flanked by I-*Sce*I sites was amplified from pGSKU using SIP2 3Q-R CORE UP45 and SIP2 3Q-R CORE DN45 v2 and transformed in destination strains. These were transformed with pRS413 containing an *Eag*I-*Sac*I fragment of *SIP2* with the *sip2*^{3R} or *sip2*^{3Q} sequences, then cells plated on YPGal then FOA. *snf1*^{L183I} and *snf1*^{T210D} were introduced by CRISPR as described [116].

All cells were grown in YPD media (2% peptone, 1% yeast extract, 2% glucose) at 30°C with shaking at 200 rpm. Media components were purchased from Formedium and media was sterilised by filtration. MEP experiments were performed as described with modifications [117]: cells were inoculated in 4 ml YPD and grown for 6-8 hours then diluted in 25 ml YPD and grown for 16-18 hours to 0.2-0.6x10^7 cells/ml in 50 ml Erlenmeyer flasks. 0.125x10^7 cells per aged culture were harvested by centrifugation (15 s at 13,000 g), washed twice with 125 µl PBS and re-suspended in 125 µl of PBS containing ~3 mg/ml Biotin-NHS (Pierce 10538723). Cells were incubated for 30 min on a wheel at room temperature, washed once with 125 µl PBS and re-suspended in 125 µl YPD then inoculated in 125 ml YPD at 1x10^4 cells/ml in a 250 ml Erlenmeyer flask (FisherBrand FB33132) sealed with Parafilm. 1 µM β-estradiol (from stock of 1 mM Sigma E2758 in ethanol) was added after 1.5h. An additional 0.125x10^7 cells were harvested from the

log phase culture while biotin labelling reactions were incubating at room temperature. Cells were harvested by centrifugation for 1 min, 4600 rpm, immediately fixed by resuspension in 70% ethanol and stored at -80°C. To minimise fluorophore bleaching in culture, the window of the incubator was covered with aluminium foil, lights on the laminar flow hood were not used during labelling and tubes were covered with aluminium foil during biotin incubation. Lifespan assays in the MEP background were performed as previously described [117,118].

Cell purification

Percoll gradients (1-2 per sample depending on harvest density) were formed by vortexing 1 ml Percoll (Sigma P1644) with 110 µl 10x PBS in 2 ml tubes and centrifuging 15 min at 15,000 g, 4 °C. Ethanol fixed cells were defrosted and washed once with 1 volume of cold PBSE (PBS + 2 mM EDTA) before resuspension in ~100 µl cold PBSE per gradient and layering on top of the pre-formed gradients. Gradients were centrifuged for 4 min at 2,000 g, 4 °C, then the upper phase and brown layer of cell debris removed and discarded. 1 ml PBSE was added, mixed by inversion and centrifuged 1 min at 2,000 g, 4 °C to pellet the cells, which were then re-suspended in 1 ml PBSE per time point (re-uniting samples where split across two gradients). 25 µl Streptavidin microbeads (Miltenyi Biotech 1010007) were added and cells incubated for 5 min on a wheel at room temperature. Meanwhile, 1 LS column per sample (Miltenyi Biotech 1050236) was loaded on a QuadroMACS magnet and equilibrated with cold PBSE in 4 °C room. Cells were loaded on columns and allowed to flow through under gravity, washed with 1 ml cold PBSE and eluted with 1 ml PBSE using plunger. Cells were re-loaded on the same columns after re-equilibration with ~500 µl PBSE, washed and re-eluted, and this process repeated for a total of three successive purifications. After addition of Triton X-100 to 0.01% to aid pelleting, cells were split into 2 fractions in 1.5 ml tubes, pelleted 30 s at 20,000 g, 4 °C, frozen on N2 and stored at -70 °C.

Fitness assays

For live purification, cells were pelleted, washed twice with synthetic complete 2% glucose media, then resuspended in 2 ml final volume of the same media and incubated for 5 min on a rotating wheel with 10 µl MyOne streptavidin magnetic beads (ThermoFisher), isolated using a magnet and washed five times with 1 ml of the same media. Cells were streaked on a YPD plate and individual cells moved to specific locations using a Singer MSM400 micromanipulator. Colony size was measured 24 hours later on the screen of the micromanipulator imaging with a 4x objective, sizes were calibrated using a haemocytometer.

RNA extraction

Cells were re-suspended in 50 µl Lysis/Binding Buffer (from mirVANA kit, Life Technologies AM1560), and 50 µl 0.5 µm zirconium beads (Thistle Scientific 11079105Z) added. Cells were lysed with 5 cycles of 30 s 6500 ms^{-1} / 30 s on ice in Next Advance Bullet Blender Storm 24 (ThermoFisher) in cold room, then 250 µl Lysis/Binding buffer was added followed by 15 µl miRNA Homogenate Additive and cells were briefly vortexed before incubating for 10 minutes on ice. 300 µl acid phenol : chloroform was added, vortexed and centrifuged 5 min at 13,000 g at room temperature before extraction of the upper phase. 400 µl room temperature ethanol and 2

µl glycogen (Sigma G1767) were added and mixture incubated for 1 hour at -30 °C before centrifugation for 15 minutes at 20,000 g, 4 °C. The pellet was washed with cold 70% ethanol and re-suspended in 10 µl water. 1 µl RNA was glyoxylated and analysed on a BPTE mini-gel, and RNA was quantified using a Qubit RNA HS Assay Kit.

150 ng RNA was used to prepare libraries using the NEBNext Ultra II Directional mRNA-seq kit with poly(A)+ purification module (NEB E7760, E7490) as described with modifications: Reagent volumes for elution from poly(T) beads, reverse transcription, second strand synthesis, tailing and adaptor ligation were reduced by 50%; libraries were amplified for 13 cycles using 2 µl each primer per 50 µl reaction before two rounds of AMPure bead purification at 0.9x and elution in 11 µl 0.1x TE prior to quality control using a Bioanalyzer HS DNA ChIP (Agilent) and quantification using a KAPA Library Quantification Kit (Roche).

Sequencing and bioinformatics

Libraries were sequenced by the Babraham Institute Sequencing Facility using a NextSeq 500 instrument in 75 bp single end mode. After adapter and quality trimming using Trim Galore (v0.6.6), RNA-seq data was mapped to yeast genome R64-1-1 using HISAT2 v2.1.0 [119] by the Babraham Institute Bioinformatics Facility. Mapped data was imported into SeqMonk v1.47.0 (https://www.bioinformatics.babraham.ac.uk/projects/seqmonk/) and quantified for $\log_2$ total reads mapping to the antisense strand of annotated open reading frames (opposite strand specific libraries), excluding the mtDNA and the rDNA locus. Read counts were adjusted by Size Factor normalisation for the full set of quantified probes [120].

GO analysis of individual clusters performed using GOrilla (http://cbl-gorilla.cs.technion.ac.il/) [121]. Quoted p-values for GO analysis are FDR-corrected according to the Benjamini and Hochberg method (q-values from the GOrilla output), for brevity only the order of magnitude rather than the full q-value is given [122].

Flow cytometry

Cell pellets were re-suspended in 240 µl PBS and 9 µl 10% triton X-100 containing 0.3 µl of 1 mg/ml Streptavidin conjugated with Alexa Fluor 647 (Life technologies) and 0.6 µl of 1 mg/ml Wheat Germ Agglutinin (WGA) conjugated with CF405S (Biotium). Cells were stained for 10 min at RT on a rotating mixer while covered with aluminium foil, washed once with 300 µl PBS containing 0.01% Triton X-100, re-suspended in 200 µl PBS and immediately subject to flow cytometry analysis on a Cytek Aurora. Cells for single colour controls were prepared in the same manner as the fully stained samples. On the Aurora, time-matched unmixing reference files were required for different ages as cell size and autofluorescence varied with age. Therefore, numerical differences in fluorescence measurements between different ages are not absolutely quantitative. Cell populations were gated on FSH-H and SSC-H to remove debris, on FSC-A and FSC-H to select for single cells, and streptavidin positive (AF647) cells were selected, all in a hierarchical manner and 10,000 events acquired. Low senescence aged populations were selected using quadrants with low GFP and high WGA.

A subset of samples was acquired on an Amnis ImageStream X Mk II with the following laser power settings: 405 = 25 mW, 488 = 180 mW, 561 = 185 mW, 642 = 5 mW, SSC = 0.3 mW. On the ImageStream, cell populations were gated for; (1) single cells based on area and aspect ratio

(>0.8), (2) in-focus cells were gated based on a gradient RMS value (>50), and (3) streptavidin positive (AF647) cells, all in a hierarchical manner and 1,000 events acquired. Before data analysis, compensation was applied according to single-colour controls and auto-generated compensation matrix, see [23] for additional parameters.

As absolute measured fluorescence intensities varied over time and between machines, median normalisation has been applied across all samples of a given age in certain datasets. Quantitative comparisons are only performed within a single age group and are therefore unaffected by these normalisations.

Statistical analysis

All statistical analysis was performed in GraphPad Prism (v10.4.1).

Acknowledgements

We would like to thank Sophie Trefely and Mark Cheong for experimental help and insightful discussions. We also thank Sophie Trefely for critical reading of the manuscript. We would like to thank Rachael Walker, Sam Thompson, and Christopher Hall of the Babraham Institute Flow Facility (Flowcyt04) for extensive experimental advice and troubleshooting. RNA-seq library sequencing and processing were performed by Babraham Institute Genomics (Geno06) and Babraham Institute Bioinformatics (Bioinf01), which receive financial support from the Institute Core Capability Grant (BBSRC CCG). Funding: JH,MU,MKAM - BBSRC (BI Epigenetics ISP; BBS/E/B/000C0523), HHM – UKRI (Horizon Europe Marie Skłodowska-Curie fellowship; EP/Y027892/1), DH - BBSRC (DTP PhD award 1947502).

References

1. Medawar, P.B. (1952). An unsolved problem of biology (Published for the college by H. K. Lewis).
2. Kirkwood, T.B. (1977). Evolution of ageing. Nature *270*, 301-304.
3. Williams, G.C. (1957). Pleiotropy, natural selection and the evolution of senescence. Evolution *11*, 398-411.
4. Stroustrup, N., Anthony, W.E., Nash, Z.M., Gowda, V., Gomez, A., Lopez-Moyado, I.F., Apfeld, J., and Fontana, W. (2016). The temporal scaling of Caenorhabditis elegans ageing. Nature *530*, 103-107. 10.1038/nature16550.
5. Zhang, W.B., Sinha, D.B., Pittman, W.E., Hvatum, E., Stroustrup, N., and Pincus, Z. (2016). Extended Twilight among Isogenic C. elegans Causes a Disproportionate Scaling between Lifespan and Health. Cell Syst *3*, 333-345 e334. 10.1016/j.cels.2016.09.003.
6. Bylino, O.V., Ogienko, A.A., Batin, M.A., Georgiev, P.G., and Omelina, E.S. (2024). Genetic, Environmental, and Stochastic Components of Lifespan Variability: The Drosophila Paradigm. Int J Mol Sci *25*. 10.3390/ijms25084482.
7. Brooks-Wilson, A.R. (2013). Genetics of healthy aging and longevity. Hum Genet *132*, 1323-1338. 10.1007/s00439-013-1342-z.
8. Li, Y., Jiang, Y., Paxman, J., O'Laughlin, R., Klepin, S., Zhu, Y., Pillus, L., Tsimring, L.S., Hasty, J., and Hao, N. (2020). A programmable fate decision landscape underlies single-cell aging in yeast. Science *369*, 325-329. 10.1126/science.aax9552.

9. Speakman, J.R., and Mitchell, S.E. (2011). Caloric restriction. Mol Aspects Med *32*, 159-221. 10.1016/j.mam.2011.07.001.
10. Osborne, T.B., Mendel, L.B., and Ferry, E.L. (1917). The Effect of Retardation of Growth Upon the Breeding Period and Duration of Life of Rats. Science *45*, 294-295. 10.1126/science.45.1160.294.
11. Colman, R.J., Anderson, R.M., Johnson, S.C., Kastman, E.K., Kosmatka, K.J., Beasley, T.M., Allison, D.B., Cruzen, C., Simmons, H.A., Kemnitz, J.W., and Weindruch, R. (2009). Caloric restriction delays disease onset and mortality in rhesus monkeys. Science *325*, 201-204. 10.1126/science.1173635.
12. Mattison, J.A., Roth, G.S., Beasley, T.M., Tilmont, E.M., Handy, A.M., Herbert, R.L., Longo, D.L., Allison, D.B., Young, J.E., Bryant, M., et al. (2012). Impact of caloric restriction on health and survival in rhesus monkeys from the NIA study. Nature *489*, 318-321. 10.1038/nature11432.
13. Mannick, J.B., and Lamming, D.W. (2023). Targeting the biology of aging with mTOR inhibitors. Nat Aging *3*, 642-660. 10.1038/s43587-023-00416-y.
14. Huang, J., Kwok, A.J., Li, J.C.Y., Chiu, C.L.H., Ip, B.Y., Tung, L.Y., Zheng, X., Chow, H.T., Lo, M.P.S., Li, Z., et al. (2024). Functional and multi-omic aging rejuvenation with GLP-1R agonism. bioRxiv, 2024.2005.2006.592653. 10.1101/2024.05.06.592653.
15. Scirica, B.M., Lincoff, A.M., Lingvay, I., Bogdanski, P., Buscemi, S., Colhoun, H., Craciun, A.E., Ezhov, M., Hardt-Lindberg, S., Kleist Jeppesen, O., et al. (2024). The Effect of Semaglutide on Mortality and COVID-19-Related Deaths: An Analysis From the SELECT Trial. J Am Coll Cardiol *84*, 1632-1642. 10.1016/j.jacc.2024.08.007.
16. Li, Z., Chen, X., Vong, J.S.L., Zhao, L., Huang, J., Yan, L.Y.C., Ip, B., Wing, Y.K., Lai, H.M., Mok, V.C.T., and Ko, H. (2021). Systemic GLP-1R agonist treatment reverses mouse glial and neurovascular cell transcriptomic aging signatures in a genome-wide manner. Commun Biol *4*, 656. 10.1038/s42003-021-02208-9.
17. Mortimer, R.K., and Johnston, J.R. (1959). Life span of individual yeast cells. Nature *183*, 1751-1752. 10.1038/1831751a0.
18. Egilmez, N.K., and Jazwinski, S.M. (1989). Evidence for the involvement of a cytoplasmic factor in the aging of the yeast Saccharomyces cerevisiae. Journal of bacteriology *171*, 37-42. 10.1128/jb.171.1.37-42.1989.
19. Fehrmann, S., Paoletti, C., Goulev, Y., Ungureanu, A., Aguilaniu, H., and Charvin, G. (2013). Aging yeast cells undergo a sharp entry into senescence unrelated to the loss of mitochondrial membrane potential. Cell reports *5*, 1589-1599. 10.1016/j.celrep.2013.11.013.
20. Morlot, S., Song, J., Leger-Silvestre, I., Matifas, A., Gadal, O., and Charvin, G. (2019). Excessive rDNA Transcription Drives the Disruption in Nuclear Homeostasis during Entry into Senescence in Budding Yeast. Cell reports *28*, 408-422 e404. 10.1016/j.celrep.2019.06.032.
21. Jin, M., Li, Y., O'Laughlin, R., Bittihn, P., Pillus, L., Tsimring, L.S., Hasty, J., and Hao, N. (2019). Divergent Aging of Isogenic Yeast Cells Revealed through Single-Cell Phenotypic Dynamics. Cell Syst *8*, 242-253 e243. 10.1016/j.cels.2019.02.002.
22. Wang, J., Sang, Y., Jin, S., Wang, X., Azad, G.K., McCormick, M.A., Kennedy, B.K., Li, Q., Wang, J., Zhang, X., et al. (2022). Single-cell RNA-seq reveals early heterogeneity during aging in yeast. Aging cell *21*, e13712. 10.1111/acel.13712.
23. Horkai, D., Hadj-Moussa, H., Whale, A.J., and Houseley, J. (2023). Dietary change without caloric restriction maintains a youthful profile in ageing yeast. PLoS Biol *21*, e3002245. 10.1371/journal.pbio.3002245.
24. Herzig, S., and Shaw, R.J. (2018). AMPK: guardian of metabolism and mitochondrial homeostasis. Nat Rev Mol Cell Biol *19*, 121-135. 10.1038/nrm.2017.95.

25. Garcia, D., and Shaw, R.J. (2017). AMPK: Mechanisms of Cellular Energy Sensing and Restoration of Metabolic Balance. Mol Cell *66*, 789-800. 10.1016/j.molcel.2017.05.032.
26. Xiao, B., Sanders, M.J., Underwood, E., Heath, R., Mayer, F.V., Carmena, D., Jing, C., Walker, P.A., Eccleston, J.F., Haire, L.F., et al. (2011). Structure of mammalian AMPK and its regulation by ADP. Nature *472*, 230-233. 10.1038/nature09932.
27. Gowans, G.J., Hawley, S.A., Ross, F.A., and Hardie, D.G. (2013). AMP is a true physiological regulator of AMP-activated protein kinase by both allosteric activation and enhancing net phosphorylation. Cell metabolism *18*, 556-566. 10.1016/j.cmet.2013.08.019.
28. Yan, Y., Mukherjee, S., Harikumar, K.G., Strutzenberg, T.S., Zhou, X.E., Suino-Powell, K., Xu, T.H., Sheldon, R.D., Lamp, J., Brunzelle, J.S., et al. (2021). Structure of an AMPK complex in an inactive, ATP-bound state. Science *373*, 413-419. 10.1126/science.abe7565.
29. Steinberg, G.R., and Hardie, D.G. (2023). New insights into activation and function of the AMPK. Nat Rev Mol Cell Biol *24*, 255-272. 10.1038/s41580-022-00547-x.
30. Salminen, A., and Kaarniranta, K. (2012). AMP-activated protein kinase (AMPK) controls the aging process via an integrated signaling network. Ageing Res Rev *11*, 230-241. 10.1016/j.arr.2011.12.005.
31. Burkewitz, K., Zhang, Y., and Mair, W.B. (2014). AMPK at the nexus of energetics and aging. Cell metabolism *20*, 10-25. 10.1016/j.cmet.2014.03.002.
32. Wierman, M.B., Maqani, N., Strickler, E., Li, M., and Smith, J.S. (2017). Caloric Restriction Extends Yeast Chronological Life Span by Optimizing the Snf1 (AMPK) Signaling Pathway. Mol Cell Biol *37*. 10.1128/MCB.00562-16.
33. Stenesen, D., Suh, J.M., Seo, J., Yu, K., Lee, K.S., Kim, J.S., Min, K.J., and Graff, J.M. (2013). Adenosine nucleotide biosynthesis and AMPK regulate adult life span and mediate the longevity benefit of caloric restriction in flies. Cell metabolism *17*, 101-112. 10.1016/j.cmet.2012.12.006.
34. Greer, E.L., Dowlatshahi, D., Banko, M.R., Villen, J., Hoang, K., Blanchard, D., Gygi, S.P., and Brunet, A. (2007). An AMPK-FOXO pathway mediates longevity induced by a novel method of dietary restriction in C. elegans. Curr Biol *17*, 1646-1656. 10.1016/j.cub.2007.08.047.
35. Martin-Montalvo, A., Mercken, E.M., Mitchell, S.J., Palacios, H.H., Mote, P.L., Scheibye-Knudsen, M., Gomes, A.P., Ward, T.M., Minor, R.K., Blouin, M.J., et al. (2013). Metformin improves healthspan and lifespan in mice. Nature communications *4*, 2192. 10.1038/ncomms3192.
36. Mair, W., Morantte, I., Rodrigues, A.P., Manning, G., Montminy, M., Shaw, R.J., and Dillin, A. (2011). Lifespan extension induced by AMPK and calcineurin is mediated by CRTC-1 and CREB. Nature *470*, 404-408. 10.1038/nature09706.
37. Ulgherait, M., Rana, A., Rera, M., Graniel, J., and Walker, D.W. (2014). AMPK modulates tissue and organismal aging in a non-cell-autonomous manner. Cell reports *8*, 1767-1780. 10.1016/j.celrep.2014.08.006.
38. Apfeld, J., O'Connor, G., McDonagh, T., DiStefano, P.S., and Curtis, R. (2004). The AMP-activated protein kinase AAK-2 links energy levels and insulin-like signals to lifespan in C. elegans. Genes Dev *18*, 3004-3009. 10.1101/gad.1255404.
39. Yang, S., Long, L.H., Li, D., Zhang, J.K., Jin, S., Wang, F., and Chen, J.G. (2015). beta-Guanidinopropionic acid extends the lifespan of Drosophila melanogaster via an AMP-activated protein kinase-dependent increase in autophagy. Aging cell *14*, 1024-1033. 10.1111/acel.12371.
40. Mohammed, I., Hollenberg, M.D., Ding, H., and Triggle, C.R. (2021). A Critical Review of the Evidence That Metformin Is a Putative Anti-Aging Drug That Enhances Healthspan

and Extends Lifespan. Front Endocrinol (Lausanne) *12*, 718942. 10.3389/fendo.2021.718942.
41. Slack, C., Foley, A., and Partridge, L. (2012). Activation of AMPK by the putative dietary restriction mimetic metformin is insufficient to extend lifespan in Drosophila. PLoS One *7*, e47699. 10.1371/journal.pone.0047699.
42. Jiang, J.C., Jaruga, E., Repnevskaya, M.V., and Jazwinski, S.M. (2000). An intervention resembling caloric restriction prolongs life span and retards aging in yeast. FASEB journal : official publication of the Federation of American Societies for Experimental Biology *14*, 2135-2137. 10.1096/fj.00-0242fje.
43. Anderson, R.M., Bitterman, K.J., Wood, J.G., Medvedik, O., and Sinclair, D.A. (2003). Nicotinamide and PNC1 govern lifespan extension by calorie restriction in Saccharomyces cerevisiae. Nature *423*, 181-185. 10.1038/nature01578.
44. Kaeberlein, M., Kirkland, K.T., Fields, S., and Kennedy, B.K. (2004). Sir2-independent life span extension by calorie restriction in yeast. PLoS Biol *2*, E296. 10.1371/journal.pbio.0020296.
45. Maqani, N., Fine, R.D., Shahid, M., Li, M., Enriquez-Hesles, E., and Smith, J.S. (2018). Spontaneous mutations in CYC8 and MIG1 suppress the short chronological lifespan of budding yeast lacking SNF1/AMPK. Microb Cell *5*, 233-248. 10.15698/mic2018.05.630.
46. Ashrafi, K., Lin, S.S., Manchester, J.K., and Gordon, J.I. (2000). Sip2p and its partner snf1p kinase affect aging in S. cerevisiae. Genes Dev *14*, 1872-1885.
47. Ghillebert, R., Swinnen, E., Wen, J., Vandesteene, L., Ramon, M., Norga, K., Rolland, F., and Winderickx, J. (2011). The AMPK/SNF1/SnRK1 fuel gauge and energy regulator: structure, function and regulation. FEBS J *278*, 3978-3990. 10.1111/j.1742-4658.2011.08315.x.
48. Simpson-Lavy, K.J., and Kupiec, M. (2022). Regulation of yeast Snf1 (AMPK) by a polyhistidine containing pH sensing module. iScience *25*, 105083. 10.1016/j.isci.2022.105083.
49. Rubenstein, E.M., McCartney, R.R., Zhang, C., Shokat, K.M., Shirra, M.K., Arndt, K.M., and Schmidt, M.C. (2008). Access denied: Snf1 activation loop phosphorylation is controlled by availability of the phosphorylated threonine 210 to the PP1 phosphatase. J Biol Chem *283*, 222-230. 10.1074/jbc.M707957200.
50. Hong, S.P., Leiper, F.C., Woods, A., Carling, D., and Carlson, M. (2003). Activation of yeast Snf1 and mammalian AMP-activated protein kinase by upstream kinases. PNAS *100*, 8839-8843. 10.1073/pnas.1533136100.
51. Nicastro, R., Tripodi, F., Gaggini, M., Castoldi, A., Reghellin, V., Nonnis, S., Tedeschi, G., and Coccetti, P. (2015). Snf1 Phosphorylates Adenylate Cyclase and Negatively Regulates Protein Kinase A-dependent Transcription in Saccharomyces cerevisiae. J Biol Chem *290*, 24715-24726. 10.1074/jbc.M115.658005.
52. Caligaris, M., Nicastro, R., Hu, Z., Tripodi, F., Hummel, J.E., Pillet, B., Deprez, M.A., Winderickx, J., Rospert, S., Coccetti, P., et al. (2023). Snf1/AMPK fine-tunes TORC1 signaling in response to glucose starvation. eLife *12*. 10.7554/eLife.84319.
53. Treitel, M.A., Kuchin, S., and Carlson, M. (1998). Snf1 protein kinase regulates phosphorylation of the Mig1 repressor in Saccharomyces cerevisiae. Mol Cell Biol *18*, 6273-6280. 10.1128/MCB.18.11.6273.
54. Charbon, G., Breunig, K.D., Wattiez, R., Vandenhaute, J., and Noel-Georis, I. (2004). Key role of Ser562/661 in Snf1-dependent regulation of Cat8p in Saccharomyces cerevisiae and Kluyveromyces lactis. Mol Cell Biol *24*, 4083-4091. 10.1128/MCB.24.10.4083-4091.2004.
55. Wellen, K.E., Hatzivassiliou, G., Sachdeva, U.M., Bui, T.V., Cross, J.R., and Thompson, C.B. (2009). ATP-citrate lyase links cellular metabolism to histone acetylation. Science *324*, 1076-1080. 10.1126/science.1164097.

56. Frost, G., Sleeth, M.L., Sahuri-Arisoylu, M., Lizarbe, B., Cerdan, S., Brody, L., Anastasovska, J., Ghourab, S., Hankir, M., Zhang, S., et al. (2014). The short-chain fatty acid acetate reduces appetite via a central homeostatic mechanism. Nature communications *5*, 3611. 10.1038/ncomms4611.
57. Schug, Z.T., Peck, B., Jones, D.T., Zhang, Q., Grosskurth, S., Alam, I.S., Goodwin, L.M., Smethurst, E., Mason, S., Blyth, K., et al. (2015). Acetyl-CoA synthetase 2 promotes acetate utilization and maintains cancer cell growth under metabolic stress. Cancer Cell *27*, 57-71. 10.1016/j.ccell.2014.12.002.
58. van den Berg, M.A., de Jong-Gubbels, P., Kortland, C.J., van Dijken, J.P., Pronk, J.T., and Steensma, H.Y. (1996). The two acetyl-coenzyme A synthetases of Saccharomyces cerevisiae differ with respect to kinetic properties and transcriptional regulation. J Biol Chem *271*, 28953-28959. 10.1074/jbc.271.46.28953.
59. Pan, D.A., and Hardie, D.G. (2002). A homologue of AMP-activated protein kinase in Drosophila melanogaster is sensitive to AMP and is activated by ATP depletion. The Biochemical journal *367*, 179-186. 10.1042/BJ20020703.
60. Munday, M.R., Campbell, D.G., Carling, D., and Hardie, D.G. (1988). Identification by amino acid sequencing of three major regulatory phosphorylation sites on rat acetyl-CoA carboxylase. Eur J Biochem *175*, 331-338. 10.1111/j.1432-1033.1988.tb14201.x.
61. Woods, A., Munday, M.R., Scott, J., Yang, X., Carlson, M., and Carling, D. (1994). Yeast SNF1 is functionally related to mammalian AMP-activated protein kinase and regulates acetyl-CoA carboxylase in vivo. J Biol Chem *269*, 19509-19515.
62. Davies, S.P., Sim, A.T., and Hardie, D.G. (1990). Location and function of three sites phosphorylated on rat acetyl-CoA carboxylase by the AMP-activated protein kinase. Eur J Biochem *187*, 183-190. 10.1111/j.1432-1033.1990.tb15293.x.
63. Neigeborn, L., and Carlson, M. (1984). Genes affecting the regulation of SUC2 gene expression by glucose repression in Saccharomyces cerevisiae. Genetics *108*, 845-858. 10.1093/genetics/108.4.845.
64. Carlson, M., Osmond, B.C., and Botstein, D. (1981). Mutants of yeast defective in sucrose utilization. Genetics *98*, 25-40. 10.1093/genetics/98.1.25.
65. Lindstrom, D.L., and Gottschling, D.E. (2009). The mother enrichment program: a genetic system for facile replicative life span analysis in Saccharomyces cerevisiae. Genetics *183*, 413-422. 10.1534/genetics.109.106229.
66. Patterson, M.N., and Maxwell, P.H. (2014). Combining magnetic sorting of mother cells and fluctuation tests to analyze genome instability during mitotic cell aging in Saccharomyces cerevisiae. Journal of visualized experiments : JoVE, e51850. 10.3791/51850.
67. Janssens, G.E., Meinema, A.C., Gonzalez, J., Wolters, J.C., Schmidt, A., Guryev, V., Bischoff, R., Wit, E.C., Veenhoff, L.M., and Heinemann, M. (2015). Protein biogenesis machinery is a driver of replicative aging in yeast. eLife *4*, e08527. 10.7554/eLife.08527.
68. Chen, C., and Contreras, R. (2007). Identifying genes that extend life span using a high-throughput screening system. Methods Mol Biol *371*, 237-248. 10.1007/978-1-59745-361-5_18.
69. Janssens, G.E., and Veenhoff, L.M. (2016). The Natural Variation in Lifespans of Single Yeast Cells Is Related to Variation in Cell Size, Ribosomal Protein, and Division Time. PLoS One *11*, e0167394. 10.1371/journal.pone.0167394.
70. Raab, A.M., Hlavacek, V., Bolotina, N., and Lang, C. (2011). Shifting the fermentative/oxidative balance in Saccharomyces cerevisiae by transcriptional deregulation of Snf1 via overexpression of the upstream activating kinase Sak1p. Applied and environmental microbiology *77*, 1981-1989. 10.1128/AEM.02219-10.
71. Garcia-Salcedo, R., Lubitz, T., Beltran, G., Elbing, K., Tian, Y., Frey, S., Wolkenhauer, O., Krantz, M., Klipp, E., and Hohmann, S. (2014). Glucose de-repression by yeast AMP-

activated protein kinase SNF1 is controlled via at least two independent steps. FEBS J *281*, 1901-1917. 10.1111/febs.12753.
72. Leupold, S., Hubmann, G., Litsios, A., Meinema, A.C., Takhaveev, V., Papagiannakis, A., Niebel, B., Janssens, G., Siegel, D., and Heinemann, M. (2019). Saccharomyces cerevisiae goes through distinct metabolic phases during its replicative lifespan. eLife *8*. 10.7554/eLife.41046.
73. Herzig, S., Raemy, E., Montessuit, S., Veuthey, J.L., Zamboni, N., Westermann, B., Kunji, E.R., and Martinou, J.C. (2012). Identification and functional expression of the mitochondrial pyruvate carrier. Science *337*, 93-96. 10.1126/science.1218530.
74. Kamei, Y., Tamada, Y., Nakayama, Y., Fukusaki, E., and Mukai, Y. (2014). Changes in transcription and metabolism during the early stage of replicative cellular senescence in budding yeast. J Biol Chem *289*, 32081-32093. 10.1074/jbc.M114.600528.
75. Yiu, G., McCord, A., Wise, A., Jindal, R., Hardee, J., Kuo, A., Shimogawa, M.Y., Cahoon, L., Wu, M., Kloke, J., et al. (2008). Pathways change in expression during replicative aging in Saccharomyces cerevisiae. The journals of gerontology. Series A, Biological sciences and medical sciences *63*, 21-34.
76. Hu, Z., Chen, K., Xia, Z., Chavez, M., Pal, S., Seol, J.H., Chen, C.C., Li, W., and Tyler, J.K. (2014). Nucleosome loss leads to global transcriptional up-regulation and genomic instability during yeast aging. Genes Dev *28*, 396-408. 10.1101/gad.233221.113.
77. Schuller, H.J. (2003). Transcriptional control of nonfermentative metabolism in the yeast Saccharomyces cerevisiae. Curr Genet *43*, 139-160. 10.1007/s00294-003-0381-8.
78. Gancedo, J.M. (1998). Yeast carbon catabolite repression. Microbiology and molecular biology reviews : MMBR *62*, 334-361. 10.1128/MMBR.62.2.334-361.1998.
79. Bojunga, N., Kotter, P., and Entian, K.D. (1998). The succinate/fumarate transporter Acr1p of Saccharomyces cerevisiae is part of the gluconeogenic pathway and its expression is regulated by Cat8p. Molecular & general genetics : MGG *260*, 453-461. 10.1007/s004380050916.
80. Lin, S.S., Manchester, J.K., and Gordon, J.I. (2001). Enhanced gluconeogenesis and increased energy storage as hallmarks of aging in Saccharomyces cerevisiae. J Biol Chem *276*, 36000-36007. 10.1074/jbc.M103509200.
81. Lesur, I., and Campbell, J.L. (2004). The transcriptome of prematurely aging yeast cells is similar to that of telomerase-deficient cells. Molecular biology of the cell *15*, 1297-1312. 10.1091/mbc.E03-10-0742.
82. van Roermund, C.W., Hettema, E.H., van den Berg, M., Tabak, H.F., and Wanders, R.J. (1999). Molecular characterization of carnitine-dependent transport of acetyl-CoA from peroxisomes to mitochondria in Saccharomyces cerevisiae and identification of a plasma membrane carnitine transporter, Agp2p. EMBO J *18*, 5843-5852. 10.1093/emboj/18.21.5843.
83. van Roermund, C.W., Elgersma, Y., Singh, N., Wanders, R.J., and Tabak, H.F. (1995). The membrane of peroxisomes in Saccharomyces cerevisiae is impermeable to NAD(H) and acetyl-CoA under in vivo conditions. EMBO J *14*, 3480-3486. 10.1002/j.1460-2075.1995.tb07354.x.
84. Swiegers, J.H., Dippenaar, N., Pretorius, I.S., and Bauer, F.F. (2001). Carnitine-dependent metabolic activities in Saccharomyces cerevisiae: three carnitine acetyltransferases are essential in a carnitine-dependent strain. Yeast *18*, 585-595. 10.1002/yea.712.
85. Shi, S., Chen, Y., Siewers, V., and Nielsen, J. (2014). Improving production of malonyl coenzyme A-derived metabolites by abolishing Snf1-dependent regulation of Acc1. mBio *5*, e01130-01114. 10.1128/mBio.01130-14.
86. Choi, J.W., and Da Silva, N.A. (2014). Improving polyketide and fatty acid synthesis by engineering of the yeast acetyl-CoA carboxylase. Journal of biotechnology *187*, 56-59. 10.1016/j.jbiotec.2014.07.430.

87. Munari, F.M., Revers, L.F., Cardone, J.M., Immich, B.F., Moura, D.J., Guecheva, T.N., Bonatto, D., Laurino, J.P., Saffi, J., Brendel, M., and Henriques, J.A. (2014). Sak1 kinase interacts with Pso2 nuclease in response to DNA damage induced by interstrand crosslink-inducing agents in Saccharomyces cerevisiae. J Photochem Photobiol B *130*, 241-253. 10.1016/j.jphotobiol.2013.11.024.
88. Lu, J.Y., Lin, Y.Y., Sheu, J.C., Wu, J.T., Lee, F.J., Chen, Y., Lin, M.I., Chiang, F.T., Tai, T.Y., Berger, S.L., et al. (2011). Acetylation of yeast AMPK controls intrinsic aging independently of caloric restriction. Cell *146*, 969-979. 10.1016/j.cell.2011.07.044.
89. Shiba, Y., Paradise, E.M., Kirby, J., Ro, D.K., and Keasling, J.D. (2007). Engineering of the pyruvate dehydrogenase bypass in Saccharomyces cerevisiae for high-level production of isoprenoids. Metabolic engineering *9*, 160-168. 10.1016/j.ymben.2006.10.005.
90. Meaden, P.G., Dickinson, F.M., Mifsud, A., Tessier, W., Westwater, J., Bussey, H., and Midgley, M. (1997). The ALD6 gene of Saccharomyces cerevisiae encodes a cytosolic, Mg(2+)-activated acetaldehyde dehydrogenase. Yeast *13*, 1319-1327. 10.1002/(SICI)1097-0061(199711)13:14<1319::AID-YEA183>3.0.CO;2-T.
91. Gross, A.S., Zimmermann, A., Pendl, T., Schroeder, S., Schoenlechner, H., Knittelfelder, O., Lamplmayr, L., Santiso, A., Aufschnaiter, A., Waltenstorfer, D., et al. (2019). Acetyl-CoA carboxylase 1-dependent lipogenesis promotes autophagy downstream of AMPK. J Biol Chem *294*, 12020-12039. 10.1074/jbc.RA118.007020.
92. Nicastro, R., Brohee, L., Alba, J., Nuchel, J., Figlia, G., Kipschull, S., Gollwitzer, P., Romero-Pozuelo, J., Fernandes, S.A., Lamprakis, A., et al. (2023). Malonyl-CoA is a conserved endogenous ATP-competitive mTORC1 inhibitor. Nat Cell Biol *25*, 1303-1318. 10.1038/s41556-023-01198-6.
93. Kawaguchi, A., Tomoda, H., Nozoe, S., Omura, S., and Okuda, S. (1982). Mechanism of action of cerulenin on fatty acid synthetase. Effect of cerulenin on iodoacetamide-induced malonyl-CoA decarboxylase activity. Journal of biochemistry *92*, 7-12. 10.1093/oxfordjournals.jbchem.a133933.
94. Gruning, N.M., Rinnerthaler, M., Bluemlein, K., Mulleder, M., Wamelink, M.M., Lehrach, H., Jakobs, C., Breitenbach, M., and Ralser, M. (2011). Pyruvate kinase triggers a metabolic feedback loop that controls redox metabolism in respiring cells. Cell metabolism *14*, 415-427. 10.1016/j.cmet.2011.06.017.
95. Beas, A.O., Gordon, P.B., Prentiss, C.L., Olsen, C.P., Kukurugya, M.A., Bennett, B.D., Parkhurst, S.M., and Gottschling, D.E. (2020). Independent regulation of age associated fat accumulation and longevity. Nature communications *11*, 2790. 10.1038/s41467-020-16358-7.
96. Lin, S.S., Manchester, J.K., and Gordon, J.I. (2003). Sip2, an N-myristoylated beta subunit of Snf1 kinase, regulates aging in Saccharomyces cerevisiae by affecting cellular histone kinase activity, recombination at rDNA loci, and silencing. J Biol Chem *278*, 13390-13397. 10.1074/jbc.M212818200.
97. Moreno, D.F., Jenkins, K., Morlot, S., Charvin, G., Csikasz-Nagy, A., and Aldea, M. (2019). Proteostasis collapse, a hallmark of aging, hinders the chaperone-Start network and arrests cells in G1. eLife *8*. 10.7554/eLife.48240.
98. Neurohr, G.E., Terry, R.L., Sandikci, A., Zou, K., Li, H., and Amon, A. (2018). Deregulation of the G1/S-phase transition is the proximal cause of mortality in old yeast mother cells. Genes Dev *32*, 1075-1084. 10.1101/gad.312140.118.
99. Lindstrom, D.L., Leverich, C.K., Henderson, K.A., and Gottschling, D.E. (2011). Replicative age induces mitotic recombination in the ribosomal RNA gene cluster of Saccharomyces cerevisiae. PLoS Genet *7*, e1002015. 10.1371/journal.pgen.1002015.
100. Zylstra, A., Hadj-Moussa, H., Horkai, D., Whale, A.J., Piguet, B., and Houseley, J. (2023). Senescence in yeast is associated with amplified linear fragments of chromosome XII

rather than ribosomal DNA circle accumulation. PLoS Biol *21*, e3002250. 10.1371/journal.pbio.3002250.
101. Huberts, D.H., Gonzalez, J., Lee, S.S., Litsios, A., Hubmann, G., Wit, E.C., and Heinemann, M. (2014). Calorie restriction does not elicit a robust extension of replicative lifespan in Saccharomyces cerevisiae. PNAS *111*, 11727-11731. 10.1073/pnas.1410024111.
102. Jo, M.C., Liu, W., Gu, L., Dang, W., and Qin, L. (2015). High-throughput analysis of yeast replicative aging using a microfluidic system. PNAS. 10.1073/pnas.1510328112.
103. Mei, S.C., and Brenner, C. (2015). Calorie restriction-mediated replicative lifespan extension in yeast is non-cell autonomous. PLoS Biol *13*, e1002048. 10.1371/journal.pbio.1002048.
104. Nestelbacher, R., Laun, P., Vondrakova, D., Pichova, A., Schuller, C., and Breitenbach, M. (2000). The influence of oxygen toxicity on yeast mother cell-specific aging. Exp Gerontol *35*, 63-70. 10.1016/s0531-5565(99)00087-x.
105. Bisschops, M.M., Vos, T., Martinez-Moreno, R., Cortes, P.T., Pronk, J.T., and Daran-Lapujade, P. (2015). Oxygen availability strongly affects chronological lifespan and thermotolerance in batch cultures of Saccharomyces cerevisiae. Microb Cell *2*, 429-444. 10.15698/mic2015.11.238.
106. Kwon, Y.Y., Lee, S.K., and Lee, C.K. (2017). Caloric Restriction-Induced Extension of Chronological Lifespan Requires Intact Respiration in Budding Yeast. Mol Cells *40*, 307-313. 10.14348/molcells.2017.2279.
107. Tuller, G., Nemec, T., Hrastnik, C., and Daum, G. (1999). Lipid composition of subcellular membranes of an FY1679-derived haploid yeast wild-type strain grown on different carbon sources. Yeast *15*, 1555-1564. 10.1002/(SICI)1097-0061(199910)15:14<1555::AID-YEA479>3.0.CO;2-Z.
108. Chen, K.L., Ven, T.N., Crane, M.M., Brunner, M.L.C., Pun, A.K., Helget, K.L., Brower, K., Chen, D.E., Doan, H., Dillard-Telm, J.D., et al. (2020). Loss of vacuolar acidity results in iron-sulfur cluster defects and divergent homeostatic responses during aging in Saccharomyces cerevisiae. Geroscience *42*, 749-764. 10.1007/s11357-020-00159-3.
109. Patnaik, P.K., Beaupere, C., Barlit, H., Romero, A.M., Tsuchiya, M., Muir, M., Martinez-Pastor, M.T., Puig, S., Kaeberlein, M., and Labunskyy, V.M. (2022). Deficiency of the RNA-binding protein Cth2 extends yeast replicative lifespan by alleviating its repressive effects on mitochondrial function. Cell reports *40*, 111113. 10.1016/j.celrep.2022.111113.
110. Altamimi, T.R., Thomas, P.D., Darwesh, A.M., Fillmore, N., Mahmoud, M.U., Zhang, L., Gupta, A., Al Batran, R., Seubert, J.M., and Lopaschuk, G.D. (2018). Cytosolic carnitine acetyltransferase as a source of cytosolic acetyl-CoA: a possible mechanism for regulation of cardiac energy metabolism. The Biochemical journal *475*, 959-976. 10.1042/BCJ20170823.
111. Fullerton, M.D., Galic, S., Marcinko, K., Sikkema, S., Pulinilkunnil, T., Chen, Z.P., O'Neill, H.M., Ford, R.J., Palanivel, R., O'Brien, M., et al. (2013). Single phosphorylation sites in Acc1 and Acc2 regulate lipid homeostasis and the insulin-sensitizing effects of metformin. Nat Med *19*, 1649-1654. 10.1038/nm.3372.
112. Houseley, J., and Tollervey, D. (2011). Repeat expansion in the budding yeast ribosomal DNA can occur independently of the canonical homologous recombination machinery. Nucleic Acids Res *39*, 8778-8791. 10.1093/nar/gkr589.
113. Janke, C., Magiera, M.M., Rathfelder, N., Taxis, C., Reber, S., Maekawa, H., Moreno-Borchart, A., Doenges, G., Schwob, E., Schiebel, E., and Knop, M. (2004). A versatile toolbox for PCR-based tagging of yeast genes: new fluorescent proteins, more markers and promoter substitution cassettes. Yeast *21*, 947-962. 10.1002/yea.1142.

114. Longtine, M.S., McKenzie, A., 3rd, Demarini, D.J., Shah, N.G., Wach, A., Brachat, A., Philippsen, P., and Pringle, J.R. (1998). Additional modules for versatile and economical PCR-based gene deletion and modification in Saccharomyces cerevisiae. Yeast *14*, 953-961.
115. Storici, F., and Resnick, M.A. (2006). The delitto perfetto approach to in vivo site-directed mutagenesis and chromosome rearrangements with synthetic oligonucleotides in yeast. Methods Enzymol *409*, 329-345. 10.1016/S0076-6879(05)09019-1.
116. Laughery, M.F., Hunter, T., Brown, A., Hoopes, J., Ostbye, T., Shumaker, T., and Wyrick, J.J. (2015). New vectors for simple and streamlined CRISPR-Cas9 genome editing in Saccharomyces cerevisiae. Yeast *32*, 711-720. 10.1002/yea.3098.
117. Cruz, C., Della Rosa, M., Krueger, C., Gao, Q., Horkai, D., King, M., Field, L., and Houseley, J. (2018). Tri-methylation of histone H3 lysine 4 facilitates gene expression in ageing cells. eLife *7*, e34081. 10.7554/eLife.34081.
118. Frenk, S., Pizza, G., Walker, R.V., and Houseley, J. (2017). Aging yeast gain a competitive advantage on non-optimal carbon sources. Aging cell *16*, 602-604. 10.1111/acel.12582.
119. Kim, D., Langmead, B., and Salzberg, S.L. (2015). HISAT: a fast spliced aligner with low memory requirements. Nat Methods *12*, 357-360. 10.1038/nmeth.3317.
120. Anders, S., and Huber, W. (2010). Differential expression analysis for sequence count data. Genome Biol *11*, R106. 10.1186/gb-2010-11-10-r106.
121. Eden, E., Navon, R., Steinfeld, I., Lipson, D., and Yakhini, Z. (2009). GOrilla: a tool for discovery and visualization of enriched GO terms in ranked gene lists. BMC bioinformatics *10*, 48. 10.1186/1471-2105-10-48.
122. Benjamini, Y., and Hochberg, Y. (1995). Controlling the False Discovery Rate - a Practical and Powerful Approach to Multiple Testing. Journal of the Royal Statistical Society Series B-Statistical Methodology *57*, 289-300. doi:10.2307/2346101.
123. Schmalix, W., and Bandlow, W. (1993). The ethanol-inducible YAT1 gene from yeast encodes a presumptive mitochondrial outer carnitine acetyltransferase. J Biol Chem *268*, 27428-27439.
124. Franken, J., Kroppenstedt, S., Swiegers, J.H., and Bauer, F.F. (2008). Carnitine and carnitine acetyltransferases in the yeast Saccharomyces cerevisiae: a role for carnitine in stress protection. Curr Genet *53*, 347-360. 10.1007/s00294-008-0191-0.

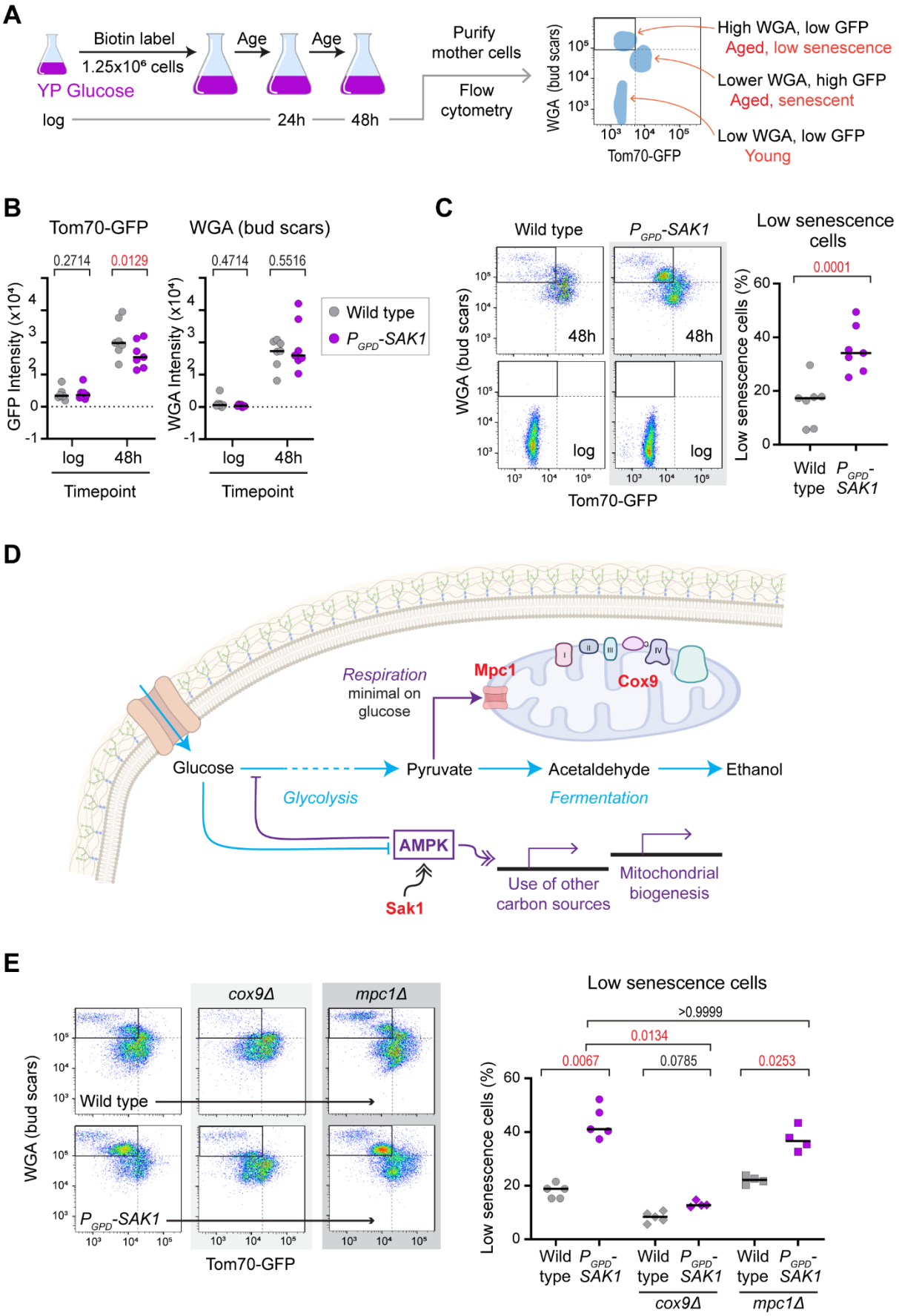
A
Biotin label
1.25x10⁶ cells
Age
Age
YP Glucose
log
24h
48h
Purify mother cells
Flow cytometry
WGA (bud scars)
Tom70-GFP
High WGA, low GFP
Aged, low senescence
Lower WGA, high GFP
Aged, senescent
Low WGA, low GFP
Young
B
Tom70-GFP
WGA (bud scars)
0.2714
0.0129
0.4714
0.5516
GFP Intensity (x10⁴)
WGA Intensity (x10⁴)
Wild type
P_GPD-SAK1
log
48h
Timepoint
C
Wild type
P_GPD-SAK1
48h
log
WGA (bud scars)
Tom70-GFP
Low senescence cells
0.0001
Low senescence cells (%)
Wild type
P_GPD-SAK1
D
Respiration
minimal on glucose
Mpc1
Cox9
Glucose
Pyruvate
Acetaldehyde
Ethanol
Glycolysis
Fermentation
AMPK
Sak1
Use of other carbon sources
Mitochondrial biogenesis
E
cox9Δ
mpc1Δ
Wild type
P_GPD-SAK1
WGA (bud scars)
Tom70-GFP
Low senescence cells
>0.9999
0.0134
0.0067
0.0785
0.0253
Low senescence cells (%)
Wild type
P_GPD-SAK1
cox9Δ
mpc1Δ

Figure 1: The impact of AMPK activation on ageing phenotypes.

A: Experimental scheme for analysis of replicatively aged yeast

B: Impact of *SAK1* overexpression on Tom70-GFP (marker of senescence onset) and WGA (marker of replicative age). p-values calculated by 2 way ANOVA, n=7

C: Separation of low senescence (high WGA low Tom70-GFP) and high senescence (low WGA high Tom70-GFP) populations by flow cytometry, and quantification of low senescence population. p-value calculated by t test, n=7

D: Simple schematic of the relationship between AMPK, mitochondria and glycolysis pathways. Central glucose processing by glycolysis leading to fermentation is shown by blue arrows, AMPK activated pathways as purple arrows. Key enzymes in this study are shown in red.

E: Representative flow plots and quantification of low senescence population in mitochondrial mutants lacking a functional electron transport chain (*cox9*Δ) or pyruvate import (*mpc1*Δ). p-values calculated by one way ANOVA, n=4-5

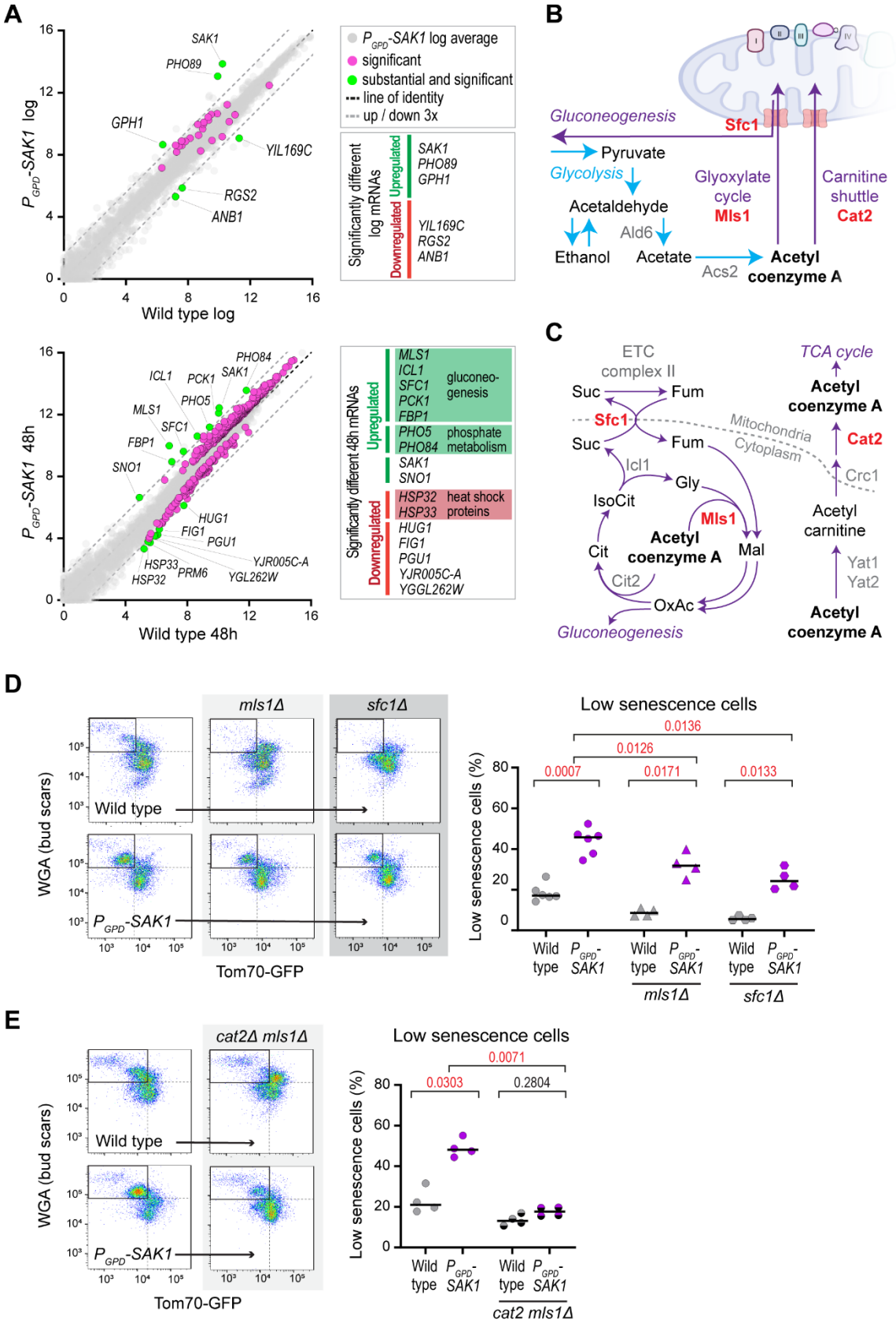
A
SAK1
PHO89
GPH1
YIL169C
RGS2
ANB1
P_GPD-SAK1 log average
significant
substantial and significant
line of identity
up / down 3x
Significantly different log mRNAs
Upregulated
Downregulated
P_GPD-SAK1 log
Wild type log
PHO84
ICL1
PCK1
SAK1
PHO5
MLS1
SFC1
FBP1
SNO1
HUG1
FIG1
PGU1
HSP33
PRM6
HSP32
YJR005C-A
YGL262W
Significantly different 48h mRNAs
gluconeo-genesis
phosphate metabolism
heat shock proteins
P_GPD-SAK1 48h
Wild type 48h
B
Gluconeogenesis
Sfc1
Pyruvate
Glycolysis
Acetaldehyde
Ald6
Ethanol
Acetate
Acs2
Acetyl coenzyme A
Glyoxylate cycle
Mls1
Carnitine shuttle
Cat2
C
ETC complex II
Suc
Fum
Sfc1
Mitochondria
Cytoplasm
Icl1
Gly
IsoCit
Mls1
Acetyl coenzyme A
Mal
Cit
Cit2
OxAc
Gluconeogenesis
TCA cycle
Acetyl carnitine
Crc1
Yat1
Yat2
D
mls1Δ
sfc1Δ
WGA (bud scars)
Wild type
P_GPD-SAK1
Tom70-GFP
Low senescence cells
Low senescence cells (%)
0.0136
0.0126
0.0007
0.0171
0.0133
Wild type
P_GPD-SAK1
mls1Δ
sfc1Δ
E
cat2Δ mls1Δ
0.0071
0.0303
0.2804
cat2 mls1Δ

Figure 2: AMPK activation reduces the SEP through acetyl coenzyme A metabolism

A: Comparison of gene expression profiles of wild type and P_{GPD}-*SAK1* cells at log phase and after 48 h ageing by mRNA-seq. Data is an average of 3 biological replicates, significantly different genes ($p<0.01$ by DEseq2) are shown in purple, genes both substantially (>3x indicated by dotted lines) and significantly different are highlighted in green. Substantially and significantly upregulated genes are annotated.

B: Schematic of the relationship between glycolysis, acetyl coenzyme A and gluconeogenesis, highlighting the degenerate pathways for entry of acetyl coenzyme A into mitochondria. Enzymes addressed in this study are highlighted in red, other selected enzymes are shown in grey.

C: Detailed schematic of the glyoxylate cycle and the cytoplasmic carnitine shuttle. Metabolites in the glyoxylate cycle: Gly - glyoxylate, Mal - malate, OxAc - oxaloacetate, Cit - citrate, IsoCit - isocitrate, Suc - succinate, Fum - fumarate, note that Sfc1 is an antiporter that exchanges succinate with fumarate. Acetyl coenzyme A enters the glyoxylate cycle at two points and exits as oxaloacetate, which is processed by Pck1 to initiate gluconeogenesis. For the carnitine shuttle, three enzymes (Cat2, Yat1, Yat2) can form acetylcarnitine of which Yat1 and Yat2 have access to cytoplasmic acetyl coenzyme A [123,124], whereas only Cat2 is present in mitochondria to regenerate acetyl coenzyme A. Enzymes addresses in this study are highlighted in red, other selected enzymes are shown in grey.

D: Representative flow plots and quantification of the low senescence population in mutants lacking the glyoxylate cycle (*mls1*Δ) or succinate import (*sfc1*Δ). p-values calculated by one way ANOVA, n=4-6

E: Representative flow plots and quantification of the low senescence population in mutants lacking both the glyoxylate cycle (*mls1*Δ) and the carnitine shuttle (*cat2*Δ). p-values calculated by one way ANOVA, n=4

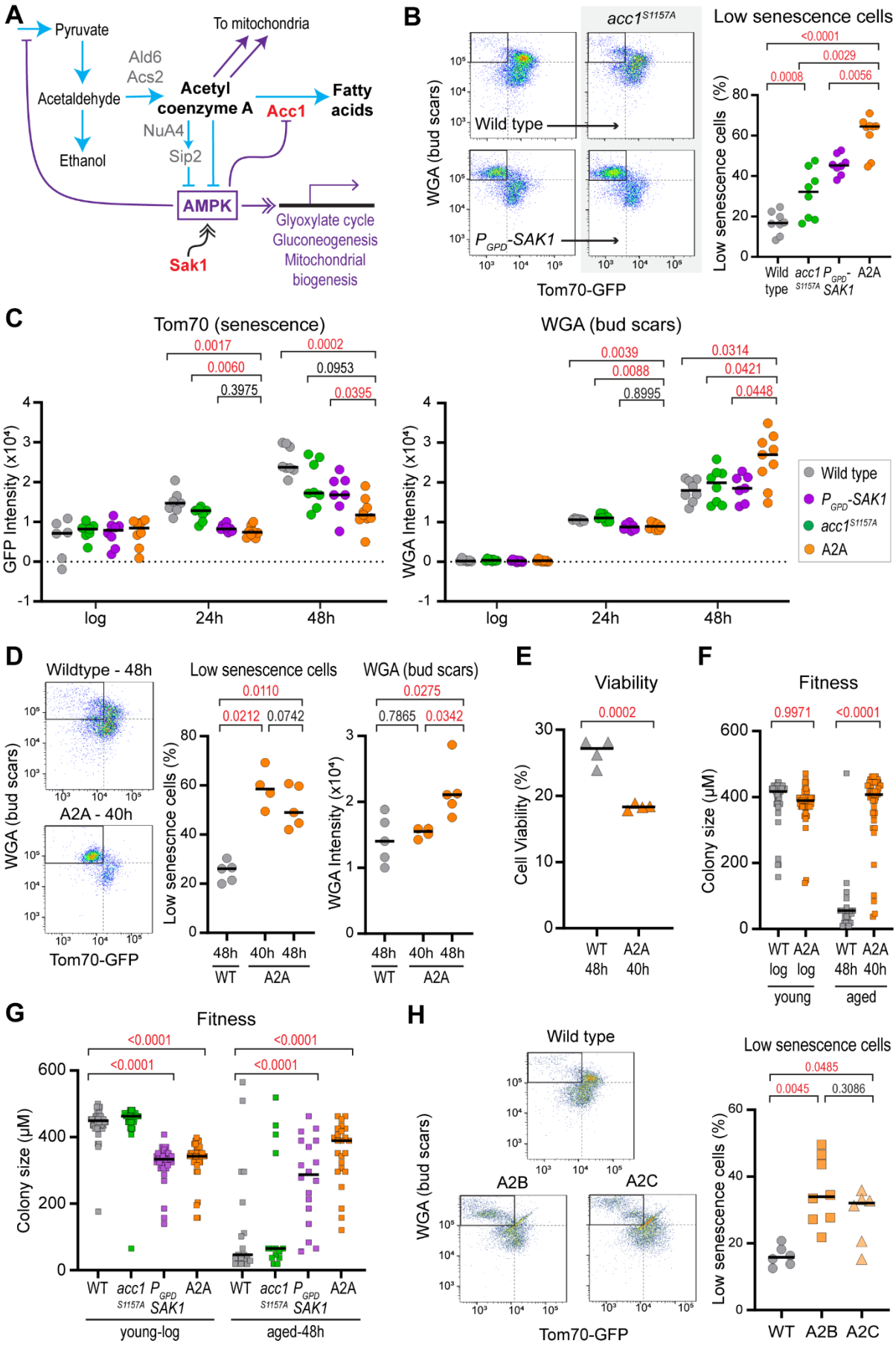
A
Pyruvate
To mitochondria
Ald6
Acs2
Acetaldehyde
Acetyl coenzyme A
Acc1
Fatty acids
NuA4
Sip2
Ethanol
AMPK
Sak1
Glyoxylate cycle
Gluconeogenesis
Mitochondrial biogenesis
B
acc1S1157A
Low senescence cells
Wild type
PGPD-SAK1
WGA (bud scars)
Tom70-GFP
Low senescence cells (%)
<0.0001
0.0029
0.0008
0.0056
Wild type
acc1 S1157A
PGPD-SAK1
A2A
C
Tom70 (senescence)
WGA (bud scars)
GFP Intensity (x10⁴)
WGA Intensity (x10⁴)
0.0017
0.0060
0.3975
0.0002
0.0953
0.0395
0.0039
0.0088
0.8995
0.0314
0.0421
0.0448
log
24h
48h
Wild type
PGPD-SAK1
acc1S1157A
A2A
D
Wildtype - 48h
A2A - 40h
WGA (bud scars)
Tom70-GFP
Low senescence cells
WGA (bud scars)
0.0110
0.0212
0.0742
0.0275
0.7865
0.0342
Low senescence cells (%)
WGA Intensity (x10⁴)
48h
40h
48h
WT
A2A
E
Viability
0.0002
Cell Viability (%)
WT 48h
A2A 40h
F
Fitness
0.9971
<0.0001
Colony size (µM)
WT log
A2A log
young
WT 48h
A2A 40h
aged
G
Fitness
<0.0001
<0.0001
<0.0001
<0.0001
Colony size (µM)
WT
acc1 S1157A
PGPD SAK1
A2A
young-log
aged-48h
H
Wild type
A2B
A2C
WGA (bud scars)
Tom70-GFP
Low senescence cells
0.0485
0.0045
0.3086
Low senescence cells (%)
WT
A2B
A2C

Figure 3: Combining AMPK activation with active fatty acid synthesis is beneficial during ageing

A: Schematic highlighting the regulation of fatty acid synthesis by AMPK.

B: Representative flow plots and quantification of the low senescence population in acc1^{S1157A}, P_{GPD}-*SAK1* and A2A. p values calculated by one way ANOVA, n=

C: Population medians for Tom70-GFP and WGA in acc1^{S1157A}, P_{GPD}-*SAK1* and A2A at log phase, 24 h and 48 h. p values calculated by two way ANOVA, n=7-9

D: Representative flow plots of wild type and A2A at matched average replicative age (48 h for wild type versus 40 h for A2A), with quantification of the low senescence population and of median WGA (bud scars). p values calculated by one way ANOVA, n=4-5

E: Percentage cell viability in cultures aged for 40 and 48 h. p value calculated by t test, n=4.

F: Size of colonies formed in 24 h on a YPD plate by log phase and age-matched wild type and A2A. Only cells that eventually formed colonies within 3 days were included to ensure all tested cells were viable. p values calculated by two way ANOVA, n=14-39

G: Size of colonies formed in 24 h on a YPD plate by log phase and 48 h-aged wild type, acc1^{S1157A}, P_{GPD}-*SAK1* and A2A. Only cells that eventually formed colonies within 3 days were included to ensure all tested cells were viable. p values calculated by two way ANOVA, n=15-61

H: Representative flow plots and quantification of the low senescence population in A2B (*snf1*^{L183} and *acc1*^{S1157A}) and A2C (*snf1*^{T210D} and *acc1*^{S1157A}). p values calculated by one way ANOVA, n= 6-8

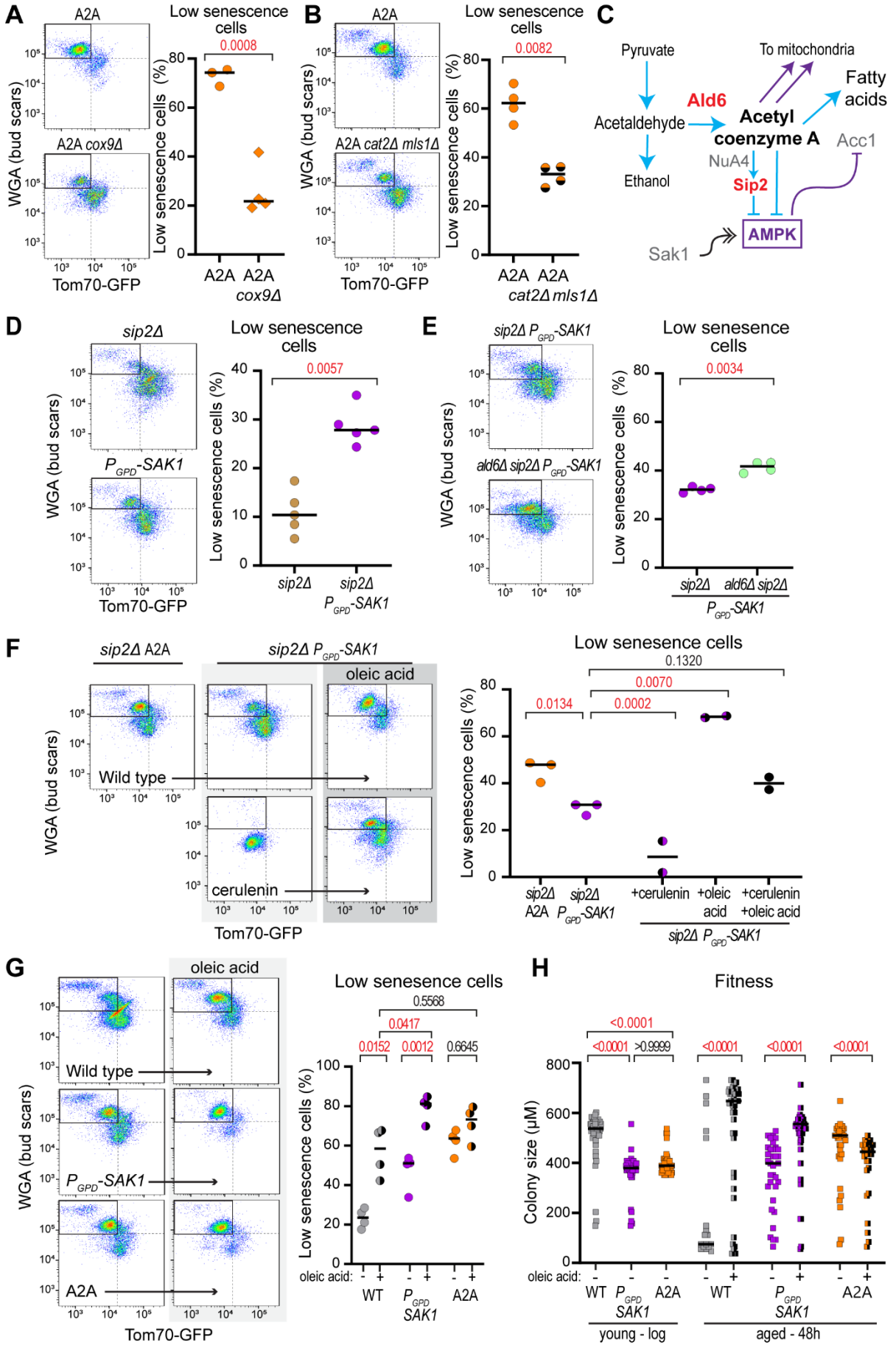
A
A2A
A2A cox9Δ
WGA (bud scars)
Tom70-GFP
Low senescence cells
0.0008
Low senescence cells (%)
A2A
A2A cox9Δ
B
A2A
A2A cat2Δ mls1Δ
WGA (bud scars)
Tom70-GFP
Low senescence cells
0.0082
Low senescence cells (%)
A2A
A2A cat2Δ mls1Δ
C
Pyruvate
To mitochondria
Fatty acids
Ald6
Acetaldehyde
Acetyl coenzyme A
Acc1
NuA4
Ethanol
Sip2
AMPK
Sak1
D
sip2Δ
P GPD-SAK1
WGA (bud scars)
Tom70-GFP
Low senescence cells
0.0057
Low senescence cells (%)
sip2Δ
sip2Δ P GPD-SAK1
E
sip2Δ P GPD-SAK1
ald6Δ sip2Δ P GPD-SAK1
WGA (bud scars)
Low senesence cells
0.0034
Low senescence cells (%)
sip2Δ
ald6Δ sip2Δ
P GPD-SAK1
F
sip2Δ A2A
sip2Δ P GPD-SAK1
oleic acid
Wild type
cerulenin
WGA (bud scars)
Tom70-GFP
Low senesence cells
0.1320
0.0070
0.0134
0.0002
Low senescence cells (%)
sip2Δ A2A
sip2Δ P GPD-SAK1
+cerulenin
+oleic acid
+cerulenin +oleic acid
sip2Δ P GPD-SAK1
G
oleic acid
Wild type
P GPD-SAK1
A2A
WGA (bud scars)
Tom70-GFP
Low senesence cells
0.5568
0.0417
0.0152
0.0012
0.6645
Low senescence cells (%)
oleic acid:
WT
P GPD SAK1
A2A
H
Fitness
<0.0001
<0.0001
>0.9999
<0.0001
<0.0001
<0.0001
Colony size (μM)
oleic acid:
WT
P GPD SAK1
A2A
young - log
aged - 48h

Figure 4: Molecular dissection of A2A phenotypes

A: Representative flow plots and quantification of healthy ageing population in A2A mutants lacking the electron transport chain (*cox9*Δ), p-values calculated by t-test, n=3-4.

B: Representative flow plots and quantification of healthy ageing population in A2A mutants lacking both the glyoxylate cycle (*mls1*Δ) and carnitine acetyltransferase activity (*cat2*Δ). p-values calculated by t-test, n=4

C: Schematic of AMPK regulation via Sip2.

D: Representative flow plots and quantification of healthy ageing population in *sip2*Δ and *sip2*Δ P_{GPD}-*SAK1*.p-values calculated by t-test, n=5

E: Representative flow plots and quantification of healthy ageing population in *sip2*Δ P_{GPD}-*SAK1* and *sip2*Δ P_{GPD}-*SAK1 ald6* Δ. p-value calculated by t-test, n=4

F: Representative flow plots and quantification of healthy ageing population in *sip2*Δ P_{GPD}-*SAK1 acc1*^{S1157A} and *sip2*Δ P_{GPD}-*SAK1* supplemented with cerulenin and/or 0.04% oleic acid + 0.04% Tween 80.p-values calculated by one-way ANOVA, n=2-3

G: Representative flow plots and quantification of healthy ageing population in wild type, P_{GPD}-*SAK1 acc1*^{S1157A} and A2A supplemented with 0.04% oleic acid + 0.04% Tween 80.p-values calculated by one-way ANOVA, n=4

H: Size of colonies formed in 24 h on a YPD plate by log phase and 48 h-aged wild type, acc1^{S1157A}, P_{GPD}-*SAK1* and A2A supplemented with 0.04% oleic acid + 0.04% Tween 80. Only cells that eventually formed colonies within 3 days were included to ensure all tested cells were viable. p values calculated by one-way ANOVA, n=19-52

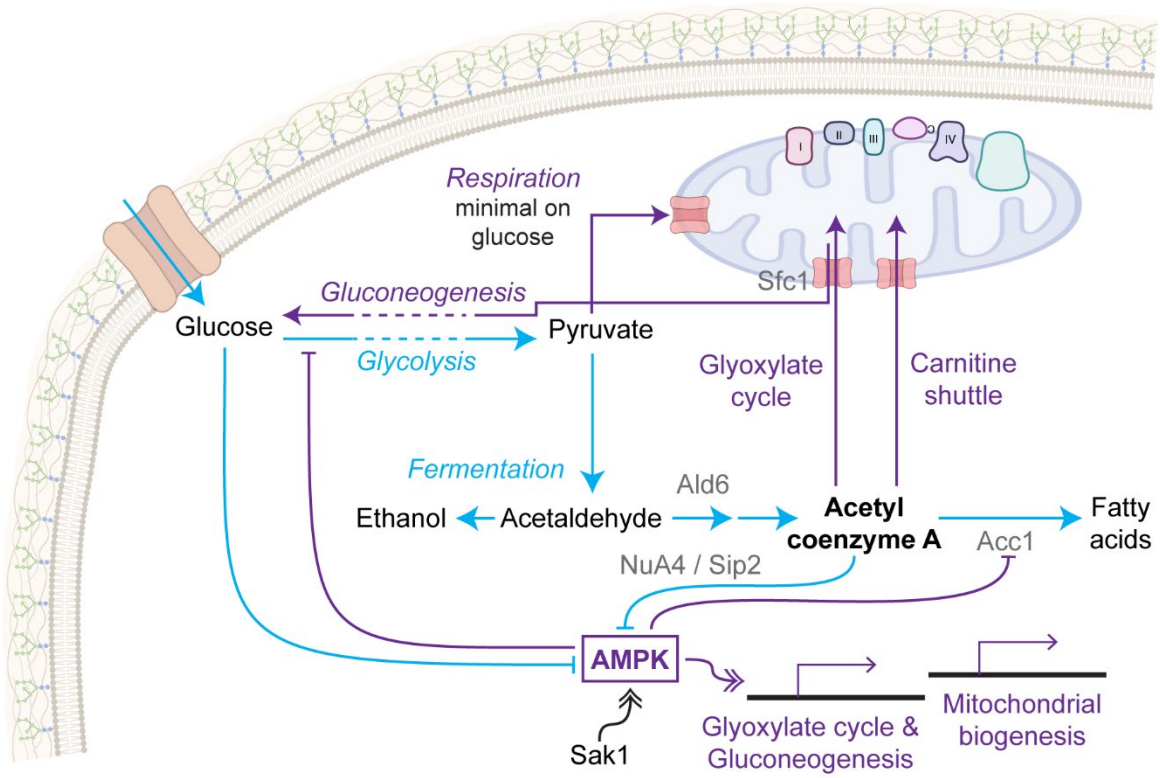

Figure 5: Metabolic pathways acting for and against senescence

Flow of glycolytic flux leading to acetyl coenzyme A (blue) and pathways promoted by AMPK (purple).

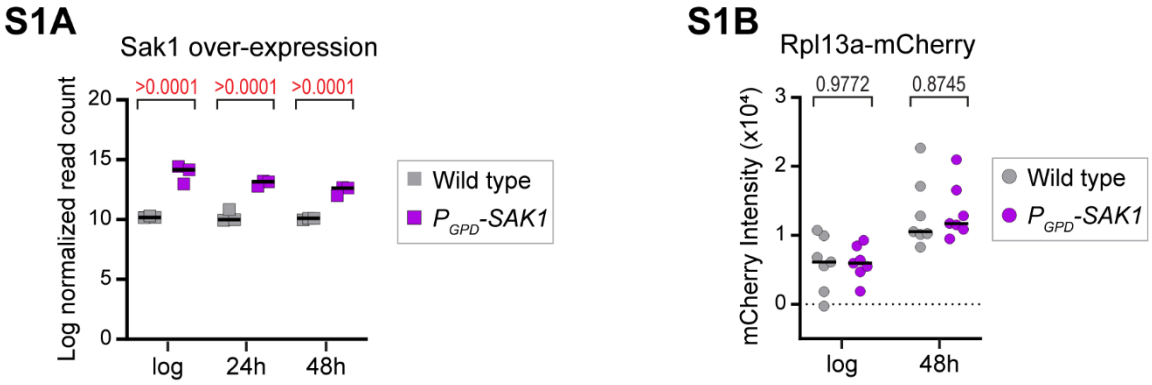

Supplementary Figure S1: The impact of AMPK activation on ageing phenotypes.

A: mRNA expression level of constitutive over-expression of the upstream kinase Sak1 using a P_{GPD} promoter fused to *SAK1* at log phase, 24 h and 48 h. p-values calculated by 1 way ANOVA, n=3

B: Impact of *SAK1* overexpression on Rpl13a-mCherry in young and aged cells. p-values calculated by 2 way ANOVA, n=7

S2A

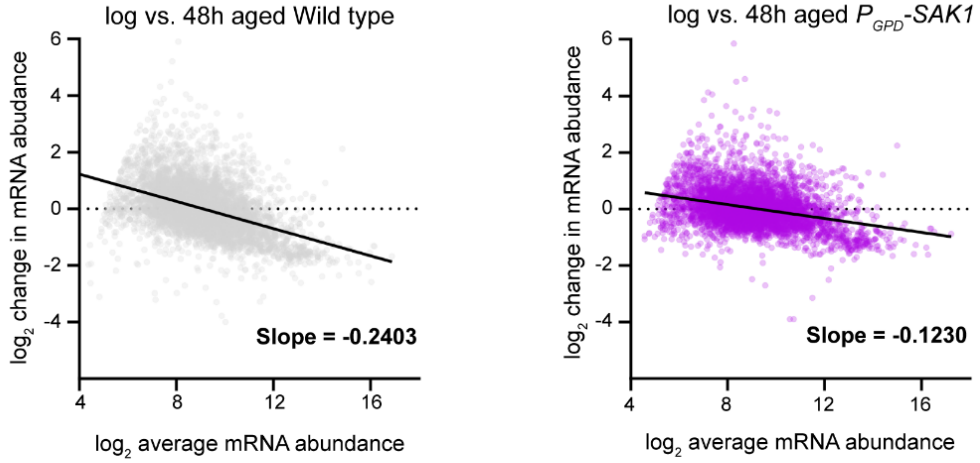

S2B

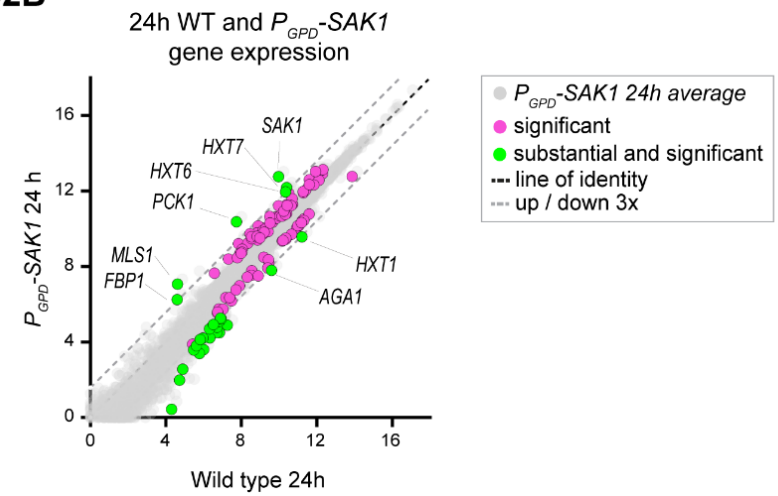

Supplementary Figure S2: AMPK activation reduces the SEP through acetyl coenzyme A metabolism

A: MA plots showing change in abundance for each mRNA between log and 48 h relative to average abundance, for wild type cells (left) and P_{GPD}-*SAK1* cells (right). Positive values on y-axis indicate increased abundance with age relative to average, negative values indicate decreased abundance, and zero indicates no change. Abundances are size factor normalised $\log_2$ transformed read counts from poly(A) selected sequencing libraries, genes with <4 counts at log phase were filtered. Data is average of 3 biological replicates, slopes calculated by linear regression.

B: Comparison of gene expression profiles of wild type and P_{GPD}-*SAK1* cells at 24 h ageing by mRNA-seq. Data is an average of 3 biological replicates, significantly different genes ($p<0.01$ by DEseq2) are shown in purple, genes both substantially (>3x indicated by dotted lines) and significantly different are highlighted in green. Substantially and significantly upregulated genes are annotated.

S3A

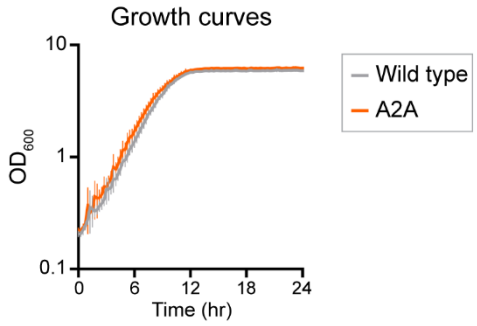

S3B

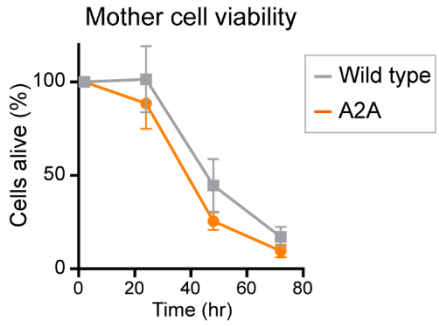

S3C

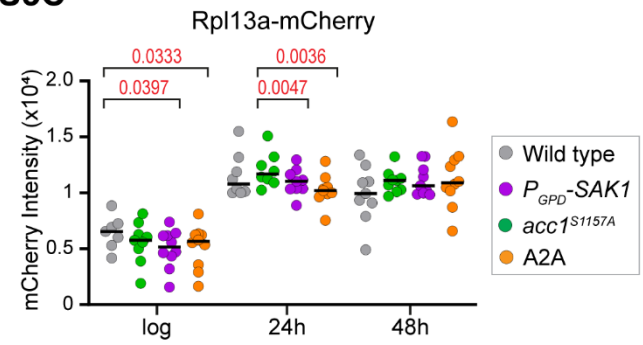

S3E

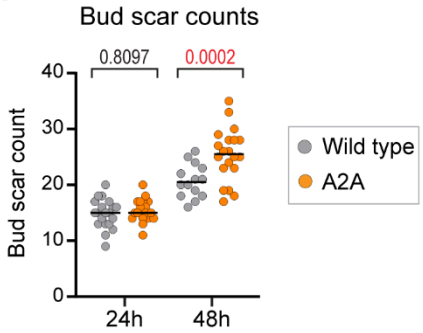

S3D

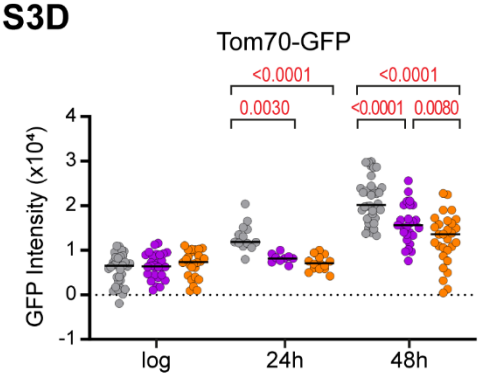

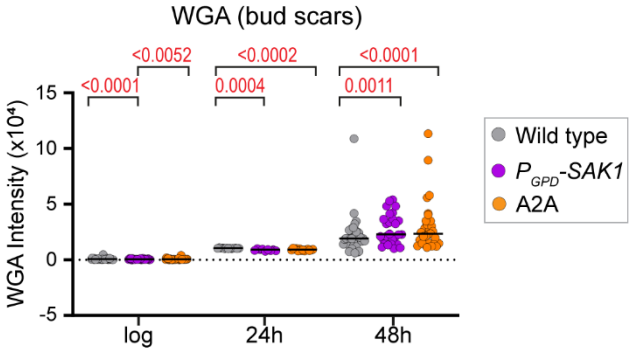

S3F

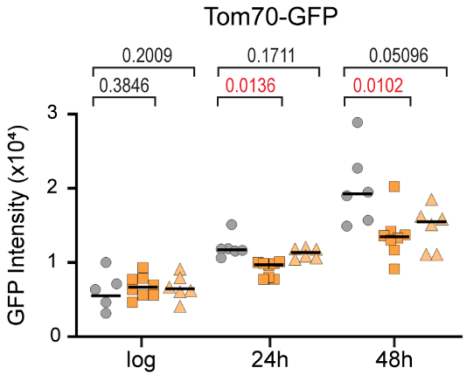

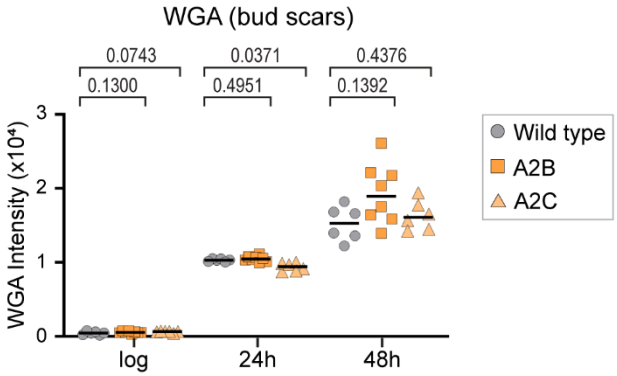

Supplementary Figure S3: Combining AMPK activation with active fatty acid synthesis is beneficial during ageing

A: Growth curve of wild type and A2A cells in YPD media starting from log-phase pre-cultures.

B: Lifespan measured in YPD media for wild type and A2A cells based on %age of viable cells remaining at each time point; *n* = 5.

C: Population medians for Rpl13a-mCherry in wild type, *acc1*^{S1157A}, P_{GPD}-*SAK1* and A2A at log phase, 24 h and 48 h. p values calculated by two way ANOVA, n=7-10.

D: Population medians for Tom70-GFP and WGA (bud scars) in wild type, P_{GPD}-*SAK1,* and A2A at log phase, 24 h and 48 h made from a compilation of experiments performed during this study. p values calculated by two way ANOVA, n=27-38.

E: Manual bud scar counts of log phase and 48 h-aged wild type and A2A cells. p values calculated by one way ANOVA, n=14-20

F: Population medians for Tom70-GFP and WGA (bud scars) in wild type, A2B (*snf1*^{L183I} *acc1*^{S1157A}) and A2C (*snf1*^{T210D} *acc1*^{S1157A}) cells at log phase, 24 h and 48 h. p values calculated by two way ANOVA, n=6-8

S4A

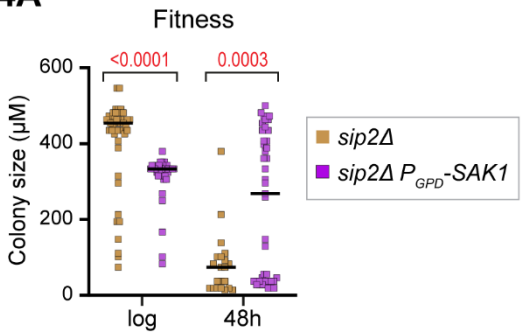

S4B

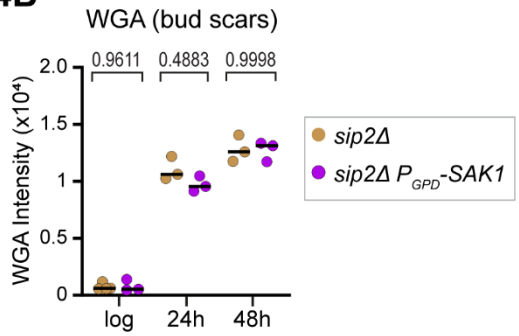

S4C

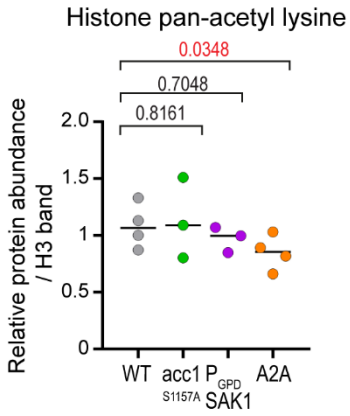

S4D

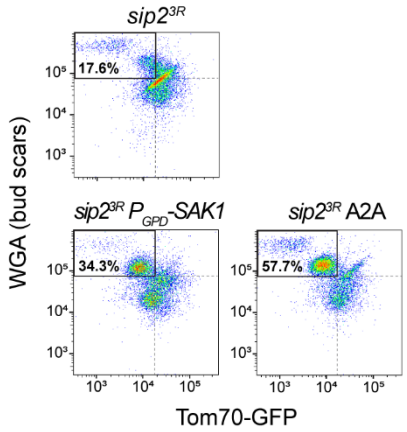

S4E

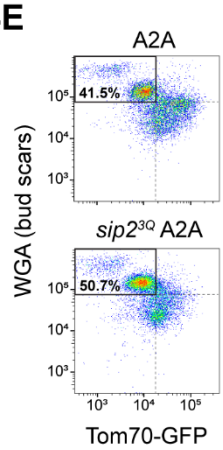

S4F

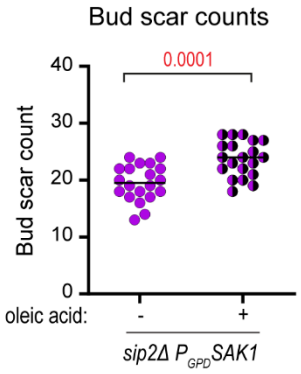

S4G

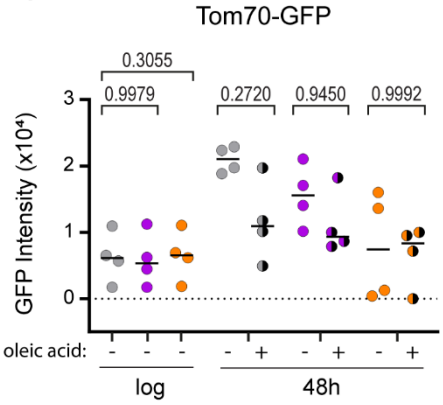

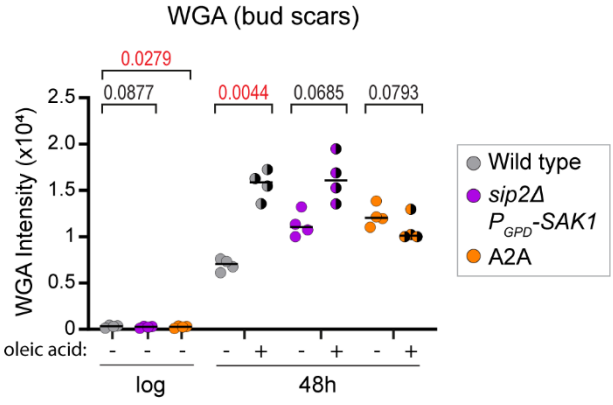

Supplementary Figure S4: Molecular dissection of A2A phenotypes

A: Size of colonies formed from individual cells in 24 h on a YPD plate by log phase and 48 h-aged *sip2*Δ and *sip2*Δ P_{GPD}-*SAK1*. Only cells that eventually formed colonies within 3 days were included to ensure all tested cells were viable. p values calculated by two-way ANOVA, n=21-46

B: Population medians for WGA (bud scars) in *sip2*Δ and *sip2*Δ P_{GPD}-*SAK1* cells at log phase, 24 h and 48 h. p values calculated by two way ANOVA, n=3-4

C: Western blot analysis of pan-acetyl lysine of H3 in log phase WT, wild type, *acc1*^{S1157A}, P_{GPD}-*SAK1* and A2A cells. Membranes were probed with mouse anti-H3 and rabbit anti-pan-acetyl lysine using a 2-colour detection system. p values calculated by one-way ANOVA, n=3-4.

D: Representative flow plots and quantification of the low senescence population in *sip2*^{3R}, *sip2*^{3R} P_{GPD}-*SAK1* and *sip2*^{3R} A2A.

E: Representative flow plots and quantification of the low senescence population in A2A and *sip2*^{3Q} A2A.

F: Manual bud scar counts of log phase and 48 h aged wild type and A2A cells. p values calculated by one way ANOVA, n=20

G: Population medians for Tom70-GFP and WGA (bud scars) in wild type, P_{GPD}-*SAK1*, A2A cells at log phase, 24 h and 48 h with and without 0.04% oleic acid + 0.04% Tween 80 supplementation. p values calculated by one way ANOVA, n=4